

Radiogenic argon diffusion studies on tw
AC .OSU no.K68 15560



Kimura, Judy T.
SOEST Library

FEB 13 1989

RETURN TO
HAWAII INSTITUTE OF GEOPHYSICS
LIBRARY ROOM

RADIOGENIC ARGON DIFFUSION STUDIES
ON TWO HAWAIIAN BASALTS

A Senior Honors Thesis
Presented to
the Faculty of the Department of Chemistry
University of Hawaii

In Partial Fulfillment
of the Requirements for the Degree
Bachelor of Science with Honors

by

Judy Tsutae Kimura

June 1968

TYPE-ERASE
5% COTTON FIBER

RESEARCH AND DEVELOPMENT DIVISION

OF THE NATIONAL BUREAU OF STANDARDS

A Senior Honor Thesis

Presented to

the Faculty of the Department of Chemistry

University of Hawaii

In partial fulfillment

of the requirements for the degree

of Bachelor of Science with Honors

by

John F. Smith

June 1968

TYPE-SET

RESEARCH DIVISION

To Dr. B, whose patient guidance made it possible

WAGLER-A
TYPE-ERASE
% COTTON FIBRE

TABLE OF CONTENTS

LIST OF TABLES	IV
LIST OF FIGURES	V
I. INTRODUCTION	1
A. Potassium-Argon Dating Method	1
B. Background of Problem	2
C. Diffusion Processes	4
II. EXPERIMENTAL	7
A. Description of Samples	7
B. Instrumentation	8
C. Gas Extraction, Purification and Analysis	11
III. RESULTS AND DISCUSSION	16
IV. SUMMARY	46
V. REFERENCES	47
VI. ACKNOWLEDGMENTS	49

CONTENTS

LIST OF PAGES

LIST OF FIGURES

I. INTRODUCTION

 a. Purpose of the Investigation

 b. Description of the Problem

 c. Literature Survey

II. EXPERIMENTAL

 a. Description of Apparatus

 b. Experimental Procedure

 c. Data and Observations

III. RESULTS AND DISCUSSION

IV. SUMMARY

V. REFERENCES

VI. ACKNOWLEDGMENTS

LIST OF TABLES

1. Data for Ar-40* Released from HK 121	17
2. Data for Ar-40* Released from Palolo	18
3. Data for Diffusion Curves for HK 121	29
4. Data for Diffusion Curves for Palolo	30
5. Data for Diffusion Curves for KAS	37
6. Fraction of Argon Released by Volume Diffusion at Different Temperatures During a 12-Hour Heating Period	41

LIST OF TABLES

1. Data for 1940* Released from the LSI 17

2. Data for 1940* Released from LSI 18

3. Data on Diffusion Curves for the LSI 29

4. Data for Diffusion Curves for LSI 30

5. Data for Diffusion Curves for LSI 32

6. Reaction of Arsenic Released by Volcanic Diffusion
at Different Concentrations During a 12-hour
Heating Period 41

TABLE
TYPE-B-RA-31
1940-1941

LIST OF FIGURES

1. Diagram of Gas Extraction, Purification and Analysis System	9
2. Plot of Fraction Released vs Time for HK 121 at 400°, 600°, 700° and 800°C.	19
3. Plot of Fraction Released vs Time for Palolo at 400°, 600° and 800°C.	20
4. Plot of Bt vs Time for HK 121 at 400°C.	21
5. Plot of Bt vs Time for HK 121 at 600° and 700°C	22
6. Plot of Bt vs Time for HK 121 at 800°C.	23
7. Plot of Bt vs Time for Palolo at 400°C.	24
8. Plot of Bt vs Time for Palolo at 600°C.	25
9. Plot of Bt vs Time for Palolo at 800°C.	26
10. Plot of Log D/a^2 vs Time for HK 121 at 400°, 600°, 700° and 800°C.	31
11. Plot of Log D/a^2 vs Time for Palolo at 400°, 600° and 800°C.	32
12. Plot of Log D/a^2 vs $1000/T^{\circ}K$ for HK 121	34
13. Plot of Log D/a^2 vs $1000/T^{\circ}K$ for Palolo	35
14. Plot of Log D/a^2 vs Time for KAS at 600°, 700° and 800°C.	38
15. Plot of Log D/a^2 vs $1000/T^{\circ}K$ for KAS.	39
16. Plot of Fraction Released in 12 Hours by Volume Diffusion vs Temperature for KAS, HK 121 and Palolo	42

LIST OF FIGURES

1.	Diagram of gas extraction, pyrolysis and analysis system	2
2.	Plot of reaction released vs time for HE I at 500°, 700° and 800°C	19
3.	Plot of reaction released vs time for I at 500°, 600° and 800°C	20
4.	Plot of $D_{1/2}$ vs time for HE I at 400°C	21
5.	Plot of $D_{1/2}$ vs time for HE I at 500° and 700°C	22
6.	Plot of $D_{1/2}$ vs time for HE I at 800°C	23
7.	Plot of $D_{1/2}$ vs time for I at 400°C	24
8.	Plot of $D_{1/2}$ vs time for I at 600°C	25
9.	Plot of $D_{1/2}$ vs time for I at 800°C	26
10.	Plot of log $D_{1/2}$ vs time for HE I at 400°, 500°, 700° and 800°C	27
11.	Plot of log $D_{1/2}$ vs time for I at 400°, 600° and 800°C	28
12.	Plot of log $D_{1/2}$ vs time for HE I	29
13.	Plot of log $D_{1/2}$ vs time for I	30
14.	Plot of log $D_{1/2}$ vs time for HE I at 500° and 700°C	31
15.	Plot of log $D_{1/2}$ vs time for I at 500° and 700°C	32
16.	Plot of reaction released in 12 hours vs volume design vs temperature for HE I and I	42

I. Introduction

A. Potassium-Argon Dating Method

The potassium-argon dating technique is based on the fact that one of the three isotopes of potassium, K-40, naturally decays to Ca-40 by β -emission and to Ar-40 by electron capture. Because the rate of decay is known, the time elapsed since the formation of a rock or mineral can be found by knowing the quantities of the parent and the daughter it contains.

This dating technique is successful because potassium is found in nearly all rocks, either as an essential constituent of the rock minerals or as a substituent or replacement atom in the lattice structure. Actually, the decay scheme to Ca-40 is not used for the age calculation because there is no convenient way to distinguish the radiogenically produced Ca-40 from the very common natural Ca-40. On the other hand, the radiogenic Ar-40 (hereafter referred to as Ar-40*) can be distinguished from the Ar-40 present in the air, as explained below.

With a knowledge of the rate of decay of K-40 to Ar-40 and Ca-40 and knowing the amounts of K-40 and Ar-40* in a sample, the following equation can be used to determine the time elapsed since the formation of a rock or mineral⁽¹⁾:

$$t = \frac{1}{\lambda_{\gamma} + \lambda_{\beta}} \ln \left[1 + \frac{\text{Ar-40}}{\text{K-40}} \left(\frac{1 + R}{R} \right) \right]$$

where t is the age of the mineral, λ_{γ} and λ_{β} are decay constants for electron capture and β -decay, respectively, and R is $\lambda_{\gamma}/\lambda_{\beta}$, the branching ratio.

Introduction

A. Kossuth's Paper on the Method

The Kossuth method being technique is based on the fact that one of the three factors of production, labor, naturally moves to the 40 by 40 position and to 40 by 40 by electric means. The rate of decay is four, the time elapsed since the formation of a rock fragment can be found by knowing the quantity of the parent and the daughter it contains.

This dating technique is successful because potassium is found in nearly all rocks, either as an essential constituent of the rock itself or as a substitution of radioactive atoms in the lattice structure. Actually, the decay scheme to 40 is not used for the age calculation because there is no convenient way to distinguish the radiocarbon produced 40 from the very common natural 40. On the other hand, the radiocarbon 14 is referred to as 14 and can be distinguished from the 40 present in the air, as explained below.

With a knowledge of the rate of decay of 14 to 14 and 40 and knowing the amount of 40 and 14 in a sample, the following equation can be used to determine the time elapsed

since the formation of a rock or mineral (1)

$$t = \frac{1}{\lambda} \ln \left(\frac{N_0}{N} \right)$$

where t is the age of the mineral, λ and A are decay constants for parent and daughter respectively, and N_0 is the number of parent atoms at the time of formation.

B. Background of Problem

From the age equation given above, rocks from the Precambrian period, as old as 2000 million years (my), have been dated⁽¹⁾. These rocks contain large amounts of radiogenic argon as compared with relatively young rocks, for example, those of the Hawaiian Islands. The latter date from those newly formed (Kilauea is currently erupting) to 20 my old.

Using the age equation, the approximate amount of Ar-40* contained in a sample of a Hawaiian rock with a potassium concentration of 2% and an age of 10 my, was calculated to be 10^{-7} cc/gm⁽²⁾. This quantity is very small but not inordinately difficult to measure with the mass spectrometric techniques now available.

The problem arises from the fact that air contains 0.934 mole percent argon with the relative isotopic abundances of 0.337 mole percent of Ar-36, 0.063 mole percent of Ar-38 and 99.600 mole percent of Ar-40⁽³⁾. It must be remembered that all substances exposed to the atmosphere adsorb air on their surfaces and in any cracks or imperfections on these surfaces. Rocks are no exception. Thus, when the rocks are heated both the radiogenic argon and the contaminating air argon are released and the Ar-40 measured is made up of both, the two parts being, of course, indistinguishable. However, knowing the ratios of the argon isotopes in air and given the fact that Ar-36 and Ar-38 occur only in the air argon, it is possible to correct for the contamination. The amount of Ar-36 which the sample contains is measured and multiplied by a factor of 296, the ratio of Ar-40 to Ar-36 in air. This means that any error in measuring the amount of Ar-36 is multiplied about 300

BACKGROUND OF PROBLEM

From the air quality survey, made from the first...
sampled, as old as 2000 million years (my), have been...
These rocks contain large amounts of radioactive argon...
as covered with relatively young rocks, for example, those of...
the Hawaiian Islands. The latter date from more newly formed...
(Hawaiian basaltic eruptions) to 20 my old.

Using the age equation, the approximate amount of ^{40}Ar - ^{39}Ar ...
contained in a sample of a Hawaiian rock with a potassium concen-...
tration of 3% and an age of 10 my, was calculated to be 10^{-10} cc/cm³...
This quantity is very small but not inordinately difficult to...
measure with the mass spectrometric techniques now available.

The problem arises from the fact that air contains 0.93%...
mole percent of ^{40}Ar - ^{39}Ar , 0.03 mole percent of ^{37}Ar - ^{39}Ar and 29.600 mole...
percent of ^{40}Ar - ^{39}Ar . It must be remembered that all substances...
exposed to the atmosphere absorb air in their surfaces and in any...
number of applications on these surfaces. Rocks are no exception.

Thus, when the rocks are heated both the radiogenic argon and the...
containing air argon are released and the ^{40}Ar - ^{39}Ar measured in...
up of both, the two gases being, of course, indistinguishable.

However, knowing the ratios of the argon isotopes in air and given...
the fact that ^{40}Ar - ^{39}Ar and ^{37}Ar - ^{39}Ar occur only in the air argon, it is...
possible to correct for the contamination. The amount of ^{40}Ar - ^{39}Ar ...
which the sample contains is assumed and multiplied by a factor...
of 100, the ratio of ^{40}Ar - ^{39}Ar in air. This means that any...
error in assuming the amount of ^{40}Ar - ^{39}Ar is multiplied about 100.

times.

By using the equation⁽⁴⁾:

$$E = \frac{ef}{100 - f}$$

where E equals percentage error in the quantity of Ar-40* due to error in Ar-36/Ar-40, e equals percentage error in Ar-36/Ar-40, and f equals percentage atmospheric argon in the sample, Funkhouser⁽⁴⁾ has shown that with 95% air argon contamination of a young rock with very little radiogenic Ar-40, a 57% error could result in the determination of the radiogenic Ar-40. Air contamination in Hawaiian rocks is commonly in the range of 70 to 90%^(4,5,6).

Much effort has been exerted to discover methods which might decrease the air contamination. Extensive diffusion studies have been undertaken by Amirkhanov⁽⁷⁾, Evernden⁽⁸⁾, Fechtig⁽⁹⁾ and others. These workers suggest preheating the sample at about 150°C to drive off as much air argon as possible without loss of a significant amount of radiogenic argon. This procedure is not entirely satisfactory because even when it was followed, the air contamination of Hawaiian rocks was still found to be from 70 to 90% by workers at the University of Hawaii^(4,5).

A technique has been suggested by Naughton⁽¹⁰⁾ which might be a useful method for more accurate Ar-40* determinations. Naughton proposed irradiating a silicate glass to produce a known quantity of Ar-39 (an isotope not found in air) and then mixing this glass with the sample to be dated. A rigorous preheating could then be used to drive off as much air argon as possible even to the extent of losing some radiogenic argon. The amount of

times

By using the equation:

$$E = \frac{100 - X}{100}$$

where E equals percentage error in the analysis of 1-500 and X is the error in 1-500/100, a equal percentage error in 1-500/100.

and E equals percentage error in the sample, (100 - 500) / 500 = 0.500, which has been shown that the air is a contamination of a young rock.

with the 1-500/100, a 500% error would result in the determination of the percentage of 1-500, air contamination in Hawaiian rocks. In common, the error is 500%.

Experiment has been carried to discover whether which might have the air contamination, because the different studies have been undertaken by Anderson (1), (2), (3) and others.

These workers suggest, repeating the sample of about 1000 to give out so much air as possible without loss of a significant amount of radioactive argon. This procedure is not entirely satisfactory because even when it was followed, the air contamination of Hawaiian rocks was still found to be from 70 to 90% by volume at the University of Hawaii (1).

A technique has been suggested by Anderson (1) which might be a useful method for some accurate 1-500 determinations. Anderson proposed treating a 1-500 sample in a vacuum a known quantity of Ar-39 (which is not found in air) and then measuring the gas with the sample to be dated. A rigorous procedure could then be used to give off as much air as possible even to the extent of losing some radioactive argon. The amount of

radiogenic argon lost could be found from the amount of Ar-39 lost by standard isotopic dilution equations. The basic assumption made in this method is that the rate of diffusion of argon from the silicate glass is similar to that of the natural rock.

An object of this research was to determine whether this assumption is reasonably valid. No diffusion measurements had yet been made on Hawaiian basalts so it was not known whether or not the diffusion rates of the Hawaiian samples are similar to those of the artificial glasses. The diffusion parameters for the artificial, irradiated silicate rocks have been previously determined⁽²⁾. The two natural (Hawaiian) samples used in this study are discussed below.

C. Diffusion Processes

Diffusion is an irreversible process by which differences in concentration are smoothed out by a flow of particles toward the area of low concentration. The basic description of the diffusion phenomenon is given by Fick's law:

$$J = -D \frac{dc}{dx}$$

where J is the flow, or diffusion current, D the diffusion coefficient and dc/dx , the concentration gradient. This relation is dependent on temperature and on the structure of the substance being studied.

By making certain assumptions, the Fick's law equation can be solved for certain physical situations. Let the structure of the substance be a sphere and the amount of argon at time zero be homogeneously distributed. Also, let the concentration of argon

radiation energy loss could be found from the amount of α - γ loss
 by standard isotopic dilution equations. The basic assumption
 was in this method is that the rate of diffusion of argon from
 the dilute glass is similar to that of the natural rock.
 An object of this research was to determine whether this
 assumption is reasonably valid. No diffusion measurements had
 been made on Hawaiian basalt so it was not known whether or
 not the diffusion rates of the Hawaiian samples are similar to
 those of the synthetic glasses. The diffusion measurements for the
 synthetic, treated silicate rocks have been previously
 determined. The two natural (Hawaiian) samples used in this
 study are discussed below.

5. Diffusion Process

Diffusion is an irreversible process by which differences
 in concentration are smoothed out by a flow of particles toward the
 area of low concentration. The basic description of the diffusion
 phenomenon is given by Fick's law:

$$J = -D \frac{dc}{dx}$$

where J is the flow, or flux, of particles, D the diffusion coeffi-
 cient and dc/dx the concentration gradient. This relation is
 dependent on temperature and on the structure of the substance
 being studied.

By making certain assumptions, the Fick's law equation can
 be solved for certain physical situations. For the structure of
 the substance as a sphere and the amount of argon it may be
 homogeneously distributed. Also, let the concentration of argon

outside the sphere equal zero. This condition can be met experimentally by adsorbing the gases released during a diffusion run on charcoal in a glass finger around which liquid nitrogen had been placed. Then the exact solution of the equation for this system is(1,11);

$$F = 1 - \frac{6}{\pi^2} \sum_{n=1}^{\infty} \frac{1}{n^2} \exp(-n^2 Bt)$$

where F is the fraction of argon lost, B is equal to $\pi^2 D/a^2$, t is time, D, the diffusion coefficient, and a the radius of the sphere.

The solution above is for high losses. A more practical (approximate) solution for low losses was found by Reichenburg(12). For values of F up to 0.85, the solution becomes,

$$F = \frac{6}{\pi^3/2} (Bt)^{\frac{1}{2}} - \frac{3}{\pi^2} (Bt)$$

or

$$\begin{aligned} Bt &= 2\pi - \frac{\pi^2 F}{3} - 2\pi (1 - \pi/3 F)^{\frac{1}{2}} \\ &= 6.28318 - 3.2899F - 6.28318 (1 - 1.0470F)^{\frac{1}{2}} \end{aligned}$$

Some complications result when a natural sample is considered. First, the shapes of naturally occurring crystals are usually only approximately spheres(1). Second, when the sample is heated at different temperatures, the simple profile is disturbed, as shown by Carslaw and Jaeger(11). Third, natural samples contain a variety of grain sizes. The grain size of a sample is usually not the sieve size and therefore if small grains, which rapidly lose their gas content, comprise a significant amount of the sample, the diffusion constants calculated would be too low(1,13).

In this study, the above were not considered to be of great significance since only relative quantities were desired. That is, the information sought was the apparent radiogenic argon loss of a typical Hawaiian rock, as compared with that of artificial silicate glasses. In addition, the grain sizes of the minerals in many Hawaiian rocks are similar. It was, however, considered important to attempt to run the diffusion analyses in a manner similar to that used for the diffusion studies of the silicate glasses⁽²⁾. The same method of heating the samples for set periods of time at known temperatures was used and the results of this study are compared with those obtained, with the hope that the data would be applicable to future work in geochronology.

EAGLE-A

TYPE-ERASE

25% COTTON FIBER

in this study, the above was not considered to be of great
importance since only relative quantities were desired. That is,
the variation sought was the apparent elongation error loss of
a typical specimen rock, as compared with that of a typical
class. In addition, the grain sizes of the minerals in many
Hawaiian rocks are similar. It was, however, considered important
to attempt to run the dilatation analysis in a manner similar to
that used for the dilatation studies of the alluvial glasses.
The same method of sectioning and sectioning for test periods of time at
many temperatures was used and the results of this study are
compared with those obtained with the data that the data would
be applicable to them in geochronology.

EXAMPLE-A
TYPE-FER-A-23
SECTION FIBER

II. Experimental

A. Description of Samples

The first sample used in this study was labeled HK 121 and is a hornblende-biotite rhyodacite from a quarry at the southwest end of Mauna Kuwale ridge, Waianae Range, Oahu. It is a massive, dark gray rock containing oligoclase phenocrysts and crystals of biotite, basaltic hornblende and magnetite in a fine-grained groundmass⁽⁴⁾. A detailed petrographic description has been published^(14,16) and a chemical analysis is reported by the Geological Survey of the United States Department of the Interior⁽¹⁵⁾. Funkhouser⁽⁴⁾ has done much work on HK 121 and shows photographs of fluid and multiple-phase inclusions contained in the rock.

Stearns and Vaksvik⁽²¹⁾ believed that this rhyodacite represented the remains of the summit of an ancient volcano. McDougall⁽⁶⁾ found support for this idea when his K-Ar dating experiments resulted in an age of 8.36 my for the rock while other rocks from the surrounding area were found to be only 2.7-3.4 my old. However, Funkhouser, after K-Ar dating of the whole rock as well as its mineral fractions, concluded that the rock is 2.3 my old and therefore contemporaneous with the rocks of the upper Waianae series, or the post-caldera flows of the Waianae range. He contended that the older age found by McDougall resulted from excess argon contained in the mineral inclusions.

This rock was selected because much work had been done on it and the total Ar-40* content was known.

The Palolo sample (HIGS-4), a coarse grained basalt, is

EXHIBIT A

Department of Geology
University of Michigan

The following is a list of the specimens which were collected at the quarry at the southwest end of Mount Royal ridge, near the base of the massive dark gray rock containing siliceous sponges and crystals of plagioclase, quartz, hornblende and magnetite in a fine-grained matrix. A detailed petrographic description has been published (1935) and a chemical analysis is reported by the Geological Survey of the United States Department of the Interior (1935).

The following work on the rock is shown by specimens of both the matrix and the sponges contained in the rock. Stearns and Van Dyke (1935) believed that this rock represents the remains of the shield of an ancient volcano. McLaughlin (1935) found support for this idea when his K-Ar dating experiments resulted in an age of 3.25 by for the rock while other rocks from the surrounding area were found to be only 2.7-2.8 by old. However, Van Dyke, Stearns, and K-Ar dating of the whole rock as well as the mineral fractions, concluded that the rocks are 2.7 by old and therefore contemporaneous with the rocks of the region. Van Dyke, Stearns, and K-Ar dating of the whole rock as well as the mineral fractions, concluded that the rocks are 2.7 by old and therefore contemporaneous with the rocks of the region. It is concluded that the age found by McLaughlin resulted from excess argon contained in the mineral fractions.

This rock was selected because much work had been done on it and the K-Ar-40 content was known.

The label reads (1935-3), a number which is

from the contact area of an intrusive body on the east face of the Palolo Quarry (Oahu) wall. A more detailed petrographic description has been published⁽¹⁴⁾, as has a chemical analysis⁽¹⁵⁾. As far as is known, no attempt to apply K-Ar dating techniques to this material has been made. This rock was selected because it is fresh and is composed of large crystals representative of the usual minerals found in Hawaiian rocks. It was believed that diffusion in these minerals would be well-defined and easily measured.

Both samples were ground to 40-60 mesh and about one-half gram was used for diffusion studies and for melting the sample in order to determine the total Ar-40* content.

B. Instrumentation

The instrumentation used in the experiments described here consisted essentially of two parts. A small all-glass, bakeable vacuum system and an all-glass mass spectrometer. Both of these have been used by many investigators and a large number of references to them may be found in the literature^(1,4,5,18,19). For this reason, a detailed description is not given but the sections are described briefly for the benefit of those completely unfamiliar with this type of equipment. A schematic diagram of the system is included as Figure 1.

The vacuum system was constructed of Pyrex tubing supported with small stainless steel clamps attached to a network of $\frac{1}{2}$ inch stainless steel rod. This grid was supported on an insulating top of Maranite (Johns Mansville & Co.). Beneath this top were

from the contact area of an intrusive body on the east face of
 the Lais Quarry (040) wall. A more detailed petrographic
 description has been published (19), and a mineral map (20).
 As far as is known, no attempt to apply K-Ar dating techniques
 to this material has been made. This work was selected because
 it is fresh and is supposed to be a typical representative of
 the recent material found in the Lais Quarry. It was believed that
 attention to these rocks would be well-warranted and easily
 rewarded.

Two samples were ground to 40-60 mesh and about one-half
 gram was used for diffusion studies and for setting the sample in
 order to determine the total K-40 content.

II. Instrumentation

The instrumentation used in the experiment is described here
 consisted essentially of two parts. A small all-glass, double
 vacuum system and an all-glass mass spectrometer. Both of these
 have been used by many investigators and a large number of references
 to them may be found in the literature (1, 2, 3, 4, 5, 6, 7, 8, 9, 10, 11, 12, 13, 14, 15, 16, 17, 18, 19, 20, 21, 22, 23, 24, 25, 26, 27, 28, 29, 30, 31, 32, 33, 34, 35, 36, 37, 38, 39, 40, 41, 42, 43, 44, 45, 46, 47, 48, 49, 50, 51, 52, 53, 54, 55, 56, 57, 58, 59, 60, 61, 62, 63, 64, 65, 66, 67, 68, 69, 70, 71, 72, 73, 74, 75, 76, 77, 78, 79, 80, 81, 82, 83, 84, 85, 86, 87, 88, 89, 90, 91, 92, 93, 94, 95, 96, 97, 98, 99, 100).
 A detailed description is not given but the essential
 described briefly for the benefit of those completely unfamiliar
 with this type of equipment. A schematic diagram of the system
 is included as Figure 1.

The vacuum system was composed of three main parts: a
 with small stainless steel clamps attached to a network of thin
 stainless steel rods. This grid was supported on an insulating top
 of stainless steel (Invarite) and a 100-ohm resistor grid was

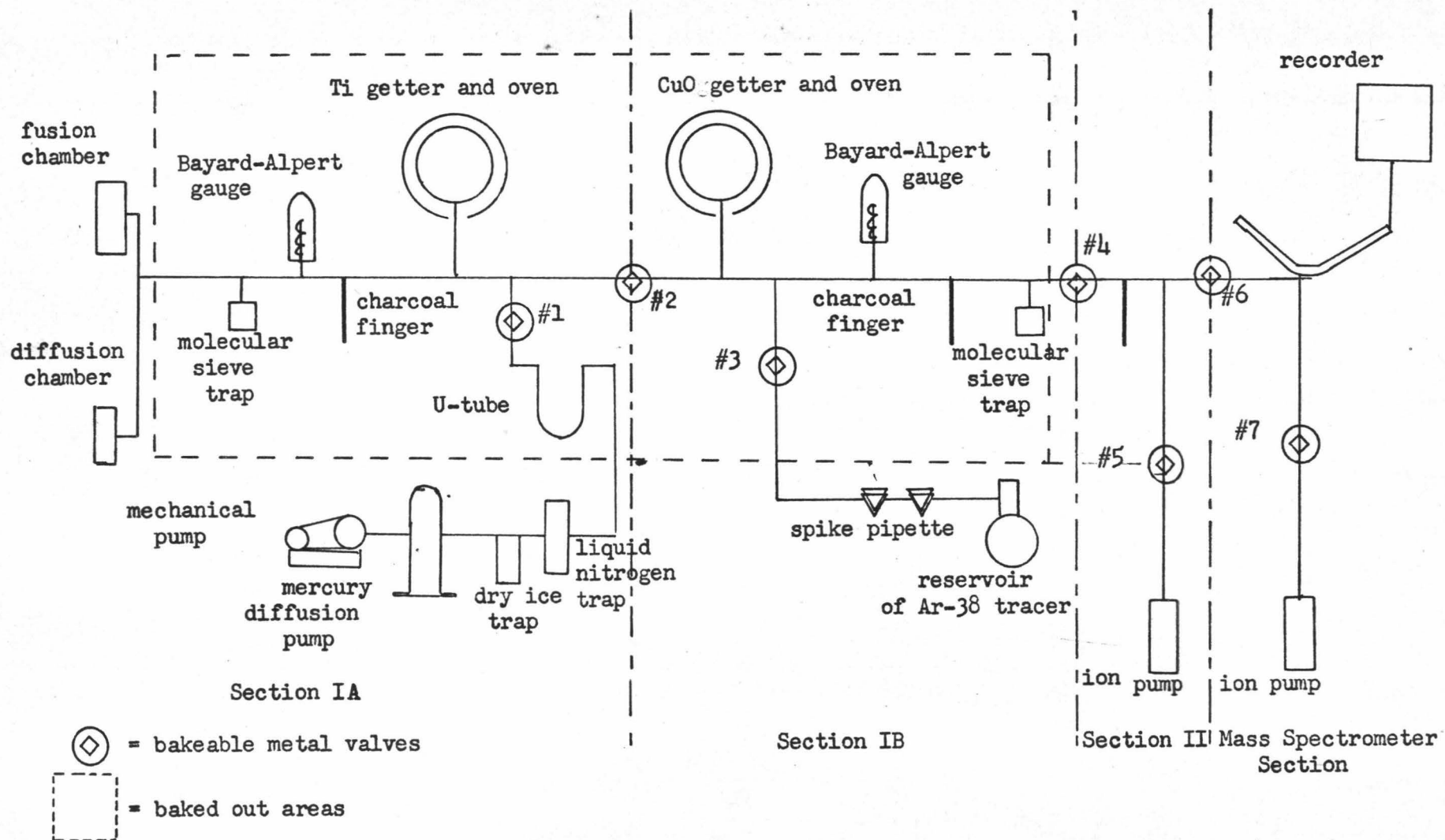


FIGURE 1 Diagram of Gas Extraction, Purification and Analysis System

a roughing pump, a mercury diffusion pump and suitable cold traps. The Ar-38 tracer addition system, similar to that described by Dalrymple⁽²²⁾ was also located below the table top.

Attached to the upper system were vacuum gauges, charcoal traps to transport the gases within the system, Ti and CuO getters for chemical purification of the gases, and molecular sieve zeolite (5A^o) traps for selective adsorption of extraneous gases. All-metal, bakeable, high vacuum valves (Granville-Phillips Co., Type C) were used to isolate various sections. This part of the upper section could be baked out at temperatures of up to 480°C.

The quartz chamber for diffusion studies and the quartz, water-jacketed fusion chambers for melting the samples were also located above the top. As explained in II.C., this section was baked out separately from the upper section described above.

The mass spectrometer used was a 4.5 inch radius, single sector, 60° magnetic deflection instrument commonly referred to as a "Reynolds-type." The entire instrument with the exception of the source and collector parts is constructed of glass with the inner surfaces of the flight tube coated with tin oxide for electrical conduction. Good detailed descriptions of this type of instrument have been published^(1,17).

In this particular instrument, the various voltages were held constant and the magnetic field varied to bring to focus on the collector slit, the ion beam of the various isotopic masses. The operating parameters used were the same as those used by Noble⁽⁵⁾;

High voltage

2 kilovolts

a roughing stage, a necessary diffusion pump and suitable cold traps, the Ar-20 tracer addition system, similar to that described by Dainton (2) was also located below the main ion.

Attached to the upper system were vacuum gauges, manual traps to transport the gases within the system, Ti and Cu gauges for chemical purification of the gases, and molecular sieve traps for selective adsorption of extremely pure gases. The Ti trap was a high vacuum valve (General Valve Co., Type 7) used to locate various sections. This part of the upper section could be baked out at temperatures of up to 800°C.

The quartz chamber for diffusion studies and the quartz water-jacketed trap chambers for waiting the samples were also located above the ion source. This section was baked out separately from the upper section described above.

The gas spectrometer used was a 100 cm radius, design sector, of magnetic deflection instrument assembly referred to as a "cyclotron type." The entire instrument with the exception of the source and collector plates is connected or fixed with the inner surface of the flight tube coated with the oxide film electrical insulation. Good detailed descriptions of this type of instrument have been published (3,4).

In this particular instrument, the various voltages were held constant and the magnetic field varied to focus on the collector slit, the ion beam of the various isotopic masses. The operating parameters used were the same as those used by

Trap current	26	microamps
Filament current	3.9	amps
Case voltage	48	volts
Case current	1.0	milliamps
Trap voltage	147	volts

C. Gas Extraction, Purification and Analysis

The procedure used maybe summarized as follows:

1. Prepared samples were placed into the quartz reaction chambers
2. Adsorbed atmospheric gases in the extraction and purification system were removed by baking out overnight under vacuum, after the reaction chambers had been attached.
3. A known amount of Ar-38 tracer was introduced into the extraction system.
4. The sample was heated for a pre-determined time and temperature for diffusion, or melted by induction heating to determine the total radiogenic Ar-40 content.
5. Released gases were purified by gettering.
6. Extracted and purified gases were analyzed mass spectrometrically.

In detail, the procedure is as follows.

For diffusion studies, the ground and weighed sample was put into the quartz diffusion chamber. For fusion work the ground and weighed samples were wrapped in aluminum foil and put into the sidearms of the reaction chambers. The chambers were glassblown onto the system and a mechanical pump was used to create a partial vacuum in order to check for leaks with a Tesla coil. If no leaks were apparent, Sections IA and IB (see Figure 1) were baked out

38
 39
 40
 41
 42

38
 39
 40
 41
 42

The reaction, purification and analysis

The procedure used was summarized as follows:

1. Prepared samples were placed into the quartz reaction

chamber

2. Absorbed atmospheric gases in the expansion and

purification system were removed by baking out overnight

under vacuum, after the reaction chamber had been attached.

3. A known amount of ^{222}Rn tracer was introduced into

the reaction system.

4. The sample was heated for a pre-determined time and

temperature for diffusion, or sealed by induction heating

to determine the total radiogenic ^{222}Rn content.

5. Released gases were purified by passing

6. Extracted and purified gases were analyzed using

electronically

In detail, the procedure is as follows:

For diffusion studies, the quartz and weighed sample was

and into a quartz diffusion chamber. The chamber was the ground

and weighed sample was weighed in a 100 mg and 100 mg

the atmosphere of the reaction chamber. The chamber was 100 mg

into the system and a mechanical pump was used to create a partial

vacuum in order to check for leaks with a leak cell. If no leaks

were observed, sections 1A and 1B (see Figure 1) were baked out

overnight at about 400°C. After degassing the molybdenum crucibles in the fusion chambers with low-level induction heating, the entire chamber was enclosed in an oven and heated to 200-330°C. The samples in the sidearm and in the diffusion chamber were heated only to 150°C, to minimize Ar-40* loss. The Ti getter was degassed at about 840°C. Bakeout was continued for 12-16 hours. During the last hour of bakeout, the exposed sections of tubing were degassed with a soft flame from a gas torch. After the ovens had cooled and been removed, the pressure was checked. Usually after bakeout, the pressure was about 4×10^{-7} torr.

Before a run, liquid nitrogen was placed on the U-tube in IA, while the Ar-38 tracer pipette was opened to the pump for 5 minutes to make certain it was clean. Then the Bayard-Alpert gauge in IB was degassed and if the pressure in the system was below 3×10^{-6} torr, valve 2 was closed for 10-15 minutes. If the pressure remained low, without substantial rise, which was an indication that the system was leak-free, a known amount of Ar-38 was introduced from the pipette. After allowing one hour to draw the spike onto the charcoal finger in IB with liquid nitrogen, valve 3 was closed and warm water (approximately 60°C) was placed around the finger.

For diffusion studies, the next step was to place a nichrome resistance wire furnace around the quartz chamber along with a chromel-alumel thermocouple for temperature measurements. Pyrex glass wool was used to cover the open ends of the furnace to prevent excessive heat loss. Air guns were used to blow cool air across the top of the diffusion furnace to prevent the quartz-to-pyrex seal from

overnight at about 160°C. After degassing the nitrogen cylinders
 in the fusion chamber with low-level radiation heater, the entire
 chamber was enclosed in an oven and heated to 200-250°C. The
 samples in the chamber and in the diffusion chamber were heated only
 to 150°C, to minimize Ar-40 loss. The Ar detector was displaced at
 about 900°C. Backout was continued for 16-18 hours. During the
 last hour of backout, the exposed sections of tubes were de-aired
 with nitrogen from a gas tank. After the oven had cooled and
 been removed, the mass was checked. Usually after backout,
 the pressure was about 1×10^{-7} torr.

Before a run, liquid nitrogen was placed on the U-tube in
 1A, while the Ar-39 tracer detector was opened to the ring for
 minutes to take constant it was taken. Then the Bayer-Albert
 gauge in 1B was degassed and all the pressure in the system was
 reduced to 1×10^{-7} torr, valve 2 was closed for 10-15 minutes. If the
 pressure remained low, without substantial rise, which was an
 indication that the system was leak-free, a known amount of Ar-39
 was introduced from the dipole. After allowing one hour to draw
 the spike into the charcoal finger in 1B with liquid nitrogen,
 valve 2 was closed and water (approximately 60°C) was placed
 around the finger.

For diffusion studies, the next step was to place a reference
 resistance wire furnace around the quartz chamber along with a
 charcoal-alumel thermocouple for temperature measurements. Pyrex
 glass wool was used to cover the open ends of the furnace to prevent
 excessive heat loss. Six tubes were used to draw cool air across the
 top of the diffusion furnace to prevent the quartz-to-glass seal from

TYPED BY ERASER

overheating and collapsing. While the sample in the diffusion chamber was being heated, liquid nitrogen was placed on the charcoal finger in IA and allowed to remain on for 20 minutes after the heating period was completed in order to catch any gas released while the sample was cooling.

The heating schedule used for the diffusion studies was similar to that used by Barnes⁽²⁾. The sample was heated for three one-hour, a two-hour and a five- to six-hour periods at 400°, 600°, 700°, and 800°C. The total time that a sample was heated at a given temperature was about 11 hours. Modifications to the schedule were made when necessary.

For fusion of a sample, a small iron bar was manipulated by a magnet to cause the foil-wrapped sample to fall into the molybdenum crucible. Then an induction coil was placed around the quartz chamber. Air was passed through the jacket of the chamber to prevent the quartz walls from overheating and air guns were used to blow cool air on the induction coils. Induction heating was continued for about six minutes at the temperature needed to melt the sample. Liquid nitrogen was placed on the charcoal finger in IA during the heating to prevent excessive buildup of gases which cause glow discharges during the heating.

After diffusion or fusion heating was completed, valve 1 was closed and the charcoal finger in IA was warmed to release the adsorbed gases. Then the Ti getter was heated for one hour at its operating temperature, 800°C. Titanium getters H₂ at 400°C and below, so valve 1 was kept closed to protect the CuO getter in IB while the Ti getter was on^(4,5). After the Ti getter had

overheating and boiling. While the sample in the distillation chamber was being heated, liquid nitrogen was placed on the chamber finger in A and allowed to remain on for 30 minutes after the heating period was completed in order to catch any gas released while the sample was cooling.

The heating schedule used for the distillation studies was similar to that used by Barnes (X). The sample was heated for three one-hour, a two-hour and a five- to six-hour periods at 400°, 500°, 700°, and 800°C. The total time that a sample was heated at a given temperature was about 12 hours. Modifications to the schedule were made when necessary.

For fusion of a sample, a small fusion bar was manipulated by a magnet to cause the following sample to fall into the nitrogen crucible. Then an induction coil was placed around the quartz chamber. Air was passed through the jacket of the chamber to prevent the quartz walls from overheating and air fans were used to blow cool air on the induction coils. Induction heating was continued for about six minutes at the temperature needed to melt the sample. Liquid nitrogen was placed on the chamber finger in A during the heating to prevent excessive heating of gas which could also be discharged during the heating.

After distillation or fusion heating was completed, valve I was closed and the chamber finger in A was wanted to release the adsorbed gases. Then the B finger was heated for one hour at its operating temperature, 500°C. Distillation returns to an 800°C and before, so valve I was kept closed to protect the B finger in the still. The B finger was cooled, and the A finger was

cooled to below 350°C, valve 1 was opened to expose the gases to the CuO getter. About 20 minutes later, the pressure of the gas sample was rapidly checked (in about 5 seconds) with the Bayard-Alpert gauge in IB. If the gauge were kept on longer, it would act as a pump and discriminately remove argon isotopes^(2,5). If the pressure was below 2×10^{-5} torr, the sample was drawn into II with liquid nitrogen on the charcoal finger in II. During the half hour allowed for this, the gaussmeter was calibrated by referencing it to mass 28 (CO + N₂), which was always present in the mass spectrometer, and the instrumental background in the region of interest was run.

When the half hour had elapsed, valve 4 was closed, the finger in II was warmed for five minutes, then valve 7 was closed and valve 6 opened for four minutes to introduce the sample into the mass spectrometer. After valve 6 had been closed for one minute to equilibrate the system, the mass spectrometric analysis was begun.

The accelerating voltage was turned on and the peaks for Ar-40, Ar-38, and Ar-36 were found and monitored for one-half to one minute intervals. Two peaks for each isotope were used to extrapolate back to zero-time in order to compensate for the "memory effect" of the instrument, which either caused the peak height to decrease or increase with time.

The time involved for the above procedure, not including the bakeout, is approximately as follows:

Physical preparation of sample	1 hour
Addition of Ar-38 tracer	1

... of the system was checked (at about 5 seconds) with the detector
... the gas. About 20 minutes later, the pressure of the gas
... was rapidly checked (at about 5 seconds) with the detector
... in the case were kept on hand, it would
... and as a check and discontinue any further work.
... the pressure was below 2 x 10⁻³ torr, the sample was drawn into
... II with liquid nitrogen on the central finger in II. During the
... half hour allowed for this, the gasometer was refilled by
... returning it to near 28 (20 + 8), which was always constant in
... the next spectrometer, and the instrumental background in the
... region of interest was zero.

... when the half hour had elapsed, valve 5 was closed, the
... finger in II was raised for five minutes, then valve 7 was closed
... and valve 6 opened for four minutes to introduce the sample into
... the next spectrometer. After valve 6 had been closed for one
... minute to equilibrate the system, the next spectrometric analysis
... was begun.

... the accelerating voltage was turned on and the peaks for
... Ar-40, Ar-38, and Ar-36 were found and measured for one-half to
... one minute intervals. Two peaks for each isotope were used as
... extrapolate back to zero time in order to compensate for the
... "memory effect" of the instrument, which either caused the peak
... height to decrease or increase with time.

... The time interval for the above procedure, not including
... the blank, is approximately as follows:
... Physical preparation of sample 1 hour
... Addition of Ar-38 tracer

Argon extraction	1 - 7
Gas purification	4
Gas analysis by mass spectrometer	1
Computation	$\frac{1}{9 - 15}$ hours

The time schedule given above is for a single time interval at one temperature. Such a schedule was repeated about 20 times each for both samples. Suggestions for reduction of this time are given below.

1 - 1
2
3
4
5
6
7 - 12 hours

APR 1954
RESEARCH
LABORATORY

The following is a list of the items which were
examined. Each item was examined about 20 times and
for both sides. Suggestions for reduction of this time are given
below.

III. Results and Discussion

As described in the introduction and experimental sections, the sample was heated at pre-determined time intervals and temperature settings. After each run, the amount of Ar-40* lost was calculated from the chart printed out by the recorder of the mass spectrometer. To find F, the sum of the Ar-40* lost during the current run and the amount lost during previous runs was divided by the total amount of Ar-40* present in the sample. The total Ar-40* content in HK 121 was found to be 2.667×10^{-7} cc/gm by Funkhouser⁽⁴⁾. Because no previous work had been done on the Palolo rock, a sample was melted and the total Ar-40* content was found to be 1.022×10^{-7} cc/gm.

From the approximation⁽¹²⁾:

$$Bt = 6.28318 - 3.2899F - 6.28318 (1 - 1.0470F)^{\frac{1}{2}}$$

the quantity Bt was found. A short computer program was written for this calculation. Tables 1 and 2 summarize the results of the experiments.

From the data in Tables 1 and 2, plots of F vs. t (time) were made. (See Figures 2 and 3) The plots for both HK 121 and Palolo show that there was a rapid loss of Ar-40* during the first three hours of heating at each temperature, after which the amount lost with time increased at a much slower rate. This rapid loss during the first few hours of heating is believed to be non-volume diffusion from at or near the surfaces, surface irregularities, grain boundaries, or structural defects. A rapid initial loss is apparent at each temperature increment probably because a rapid depletion of near surface gas takes place at the new, higher

As discussed in the Introduction and experimental sections, the sample was heated at the determined time intervals and temperature settings. After each run, the amount of weight loss was calculated from the chart plotted out by the recorder of the mass spectrometer. In Table 2, the sum of the weight loss during the experiment and the weight loss during previous runs was divided by the total amount of weight loss in the sample. The total weight loss in the sample was found to be 2.50% by the end of the experiment. In Table 3, the weight loss in the sample is compared with the weight loss in the total sample and the total weight loss was found to be 2.50% by the end of the experiment.

(12)

The results of the weight loss experiment are shown in Table 2. For this calculation, Tables 1 and 2 summarize the results of the experiments. From the data in Tables 1 and 2, plots of $\log W_t/W_0$ (line) were made. These plots are shown in Figures 1 and 2. The plots for both 100°C and 150°C show that there was a rapid loss of weight during the first three hours of heating at each temperature, after which the weight loss with time increased at a much slower rate. This rapid loss during the first few hours of heating is believed to be non-stoichiometric in nature, or structural changes, rather than a rapid decomposition of the sample. The weight loss is believed to be non-stoichiometric in nature, or structural changes, rather than a rapid decomposition of the sample.

Table 1

Data for Ar-40* Released from HK 121

Temperature (°C)	Time (hours)	Ar-40* Released (10 ⁻⁷ cc)	Cumulative Ar-40* Released (10 ⁻⁷ cc)	F, Fraction Released (10 ⁻²)	Bt (10 ⁻³)
400	1	*0.023	0.023	1.60	0.210
	2	0.0256	0.0486	3.37	0.975
	3	0.0277	0.0763	5.29	2.44
	5	0.0257	0.102	7.07	4.43
	11	0.0925	0.194	13.5	16.8
	600	1	0.0649	0.259	18.0
2		0.0258	0.285	19.8	37.6
3		0.0661	0.351	24.4	58.7
5		0.0390	0.390	27.1	73.8
11		0.0657	0.456	31.6	104
700		1	0.0538	0.510	35.4
	2	0.0269	0.537	37.2	150
	3	0.0367	0.573	39.8	175
	5	*0.39	0.612	42.5	204
	10	0.0612	0.674	46.7	255
	800	1	0.0231	0.697	48.3
2		0.0264	0.723	50.2	303
3		0.0788	0.802	55.6	393
5		0.0396	0.842	58.4	445
11		0.0808	0.922	64.0	568

Samples marked with asterisks were probably contaminated because the amount of Ar-40 released was measured to be larger than the total Ar-40* content of the sample itself. Therefore, the amounts in the table were estimated from the samples taken at similar time intervals so that the cumulative amount of Ar-40* lost would be closer to the actual amount lost.

Refer to attached and enclosed for information of the Bureau and the Commission. The Commission has approved the proposed plan for the construction of the new building for the Bureau of the Interior. The Commission has also approved the proposed plan for the construction of the new building for the Bureau of the Interior. The Commission has also approved the proposed plan for the construction of the new building for the Bureau of the Interior.

Account	Balance	Debit	Credit	Balance
401	100.00			100.00
402	100.00			100.00
403	100.00			100.00
404	100.00			100.00
405	100.00			100.00
406	100.00			100.00
407	100.00			100.00
408	100.00			100.00
409	100.00			100.00
410	100.00			100.00
411	100.00			100.00
412	100.00			100.00
413	100.00			100.00
414	100.00			100.00
415	100.00			100.00
416	100.00			100.00
417	100.00			100.00
418	100.00			100.00
419	100.00			100.00
420	100.00			100.00
421	100.00			100.00
422	100.00			100.00
423	100.00			100.00
424	100.00			100.00
425	100.00			100.00
426	100.00			100.00
427	100.00			100.00
428	100.00			100.00
429	100.00			100.00
430	100.00			100.00
431	100.00			100.00
432	100.00			100.00
433	100.00			100.00
434	100.00			100.00
435	100.00			100.00
436	100.00			100.00
437	100.00			100.00
438	100.00			100.00
439	100.00			100.00
440	100.00			100.00
441	100.00			100.00
442	100.00			100.00
443	100.00			100.00
444	100.00			100.00
445	100.00			100.00
446	100.00			100.00
447	100.00			100.00
448	100.00			100.00
449	100.00			100.00
450	100.00			100.00
451	100.00			100.00
452	100.00			100.00
453	100.00			100.00
454	100.00			100.00
455	100.00			100.00
456	100.00			100.00
457	100.00			100.00
458	100.00			100.00
459	100.00			100.00
460	100.00			100.00
461	100.00			100.00
462	100.00			100.00
463	100.00			100.00
464	100.00			100.00
465	100.00			100.00
466	100.00			100.00
467	100.00			100.00
468	100.00			100.00
469	100.00			100.00
470	100.00			100.00
471	100.00			100.00
472	100.00			100.00
473	100.00			100.00
474	100.00			100.00
475	100.00			100.00
476	100.00			100.00
477	100.00			100.00
478	100.00			100.00
479	100.00			100.00
480	100.00			100.00
481	100.00			100.00
482	100.00			100.00
483	100.00			100.00
484	100.00			100.00
485	100.00			100.00
486	100.00			100.00
487	100.00			100.00
488	100.00			100.00
489	100.00			100.00
490	100.00			100.00
491	100.00			100.00
492	100.00			100.00
493	100.00			100.00
494	100.00			100.00
495	100.00			100.00
496	100.00			100.00
497	100.00			100.00
498	100.00			100.00
499	100.00			100.00
500	100.00			100.00

For the month of January, 1911

1911

Special Agent in Charge

Table 2

Data for Ar-40* Released from Palolo

Temperature (°C)	Time (hours)	Ar-40* Released (10 ⁻⁷ cc)	Cumulative Ar-40* Released (10 ⁻⁷ cc)	F, Fraction Released (10 ⁻²)	Bt (10 ⁻³)
400	1	0.0182	0.0182	2.08	0.361
	2	0.0359	0.0541	6.18	3.35
	3	0.0400	0.0941	10.7	10.5
	5	0.0175	0.112	12.7	14.9
	10	0.0133	0.125	14.3	18.9
	600	1	0.0521	0.177	20.2
2		0.0266	0.204	23.2	53.1
3		0.0398	0.243	27.8	78.2
5		0.0114	0.255	29.1	86.5
10		0.0000	0.255	29.1	86.5
800		1	0.0379	0.293	33.4
	2	0.0377	0.330	37.7	155
	3	0.0385	0.369	42.1	200
	7	0.0376	0.406	46.4	252

TYPE-ERASE

5% COTTON FIBER

QTY	DESCRIPTION	UNIT	PRICE	TOTAL	DATE
100	TYPE-ERASE	100	1.00	100.00	10/10/50
200	TYPE-ERASE	200	1.00	200.00	10/10/50
300	TYPE-ERASE	300	1.00	300.00	10/10/50
400	TYPE-ERASE	400	1.00	400.00	10/10/50
500	TYPE-ERASE	500	1.00	500.00	10/10/50
600	TYPE-ERASE	600	1.00	600.00	10/10/50
700	TYPE-ERASE	700	1.00	700.00	10/10/50
800	TYPE-ERASE	800	1.00	800.00	10/10/50
900	TYPE-ERASE	900	1.00	900.00	10/10/50
1000	TYPE-ERASE	1000	1.00	1000.00	10/10/50

TOTAL 10000.00

10/10/50

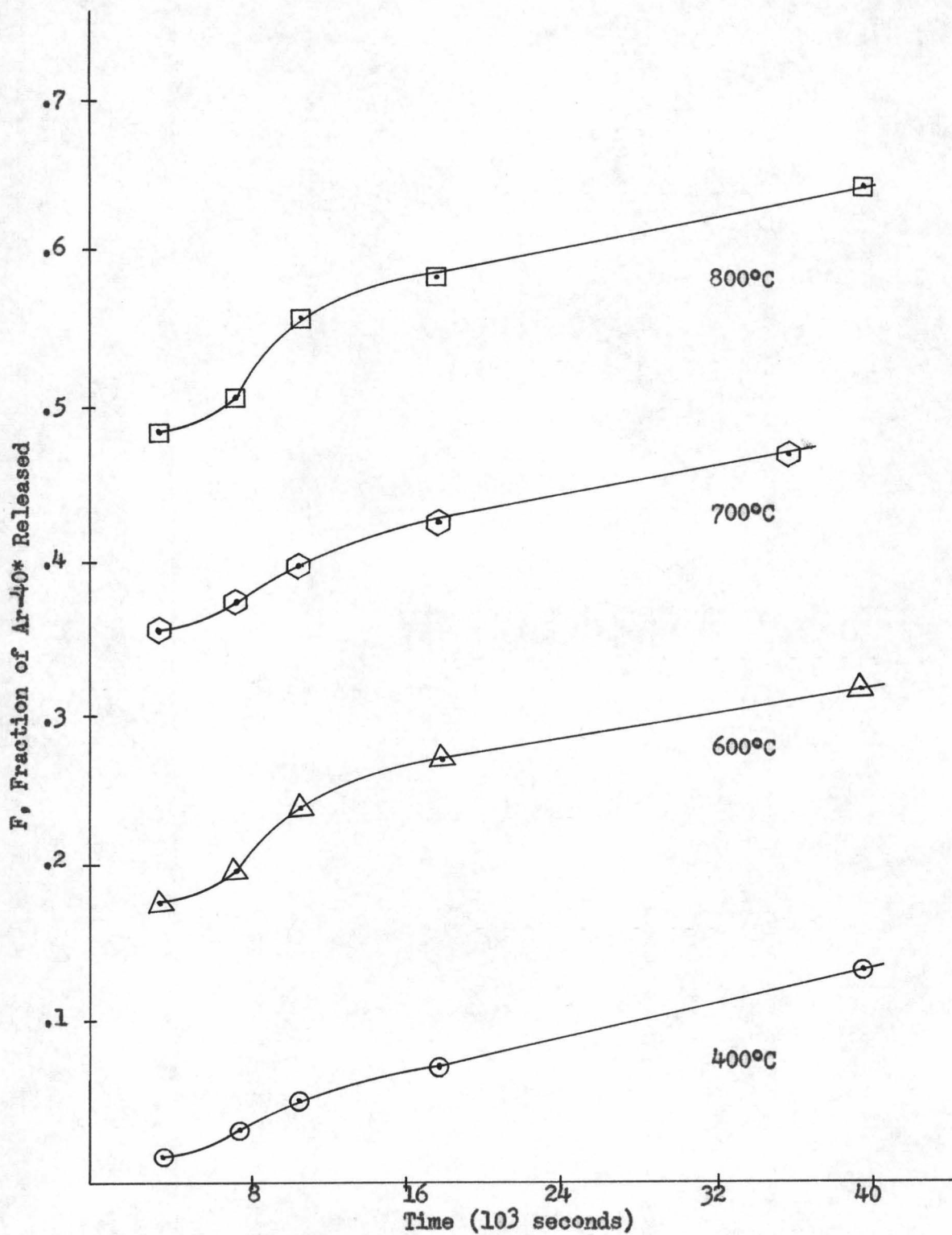


FIGURE 2 - Plot of Fraction Released vs Time for HK 121 at 400°, 600°, 700° and 800°C

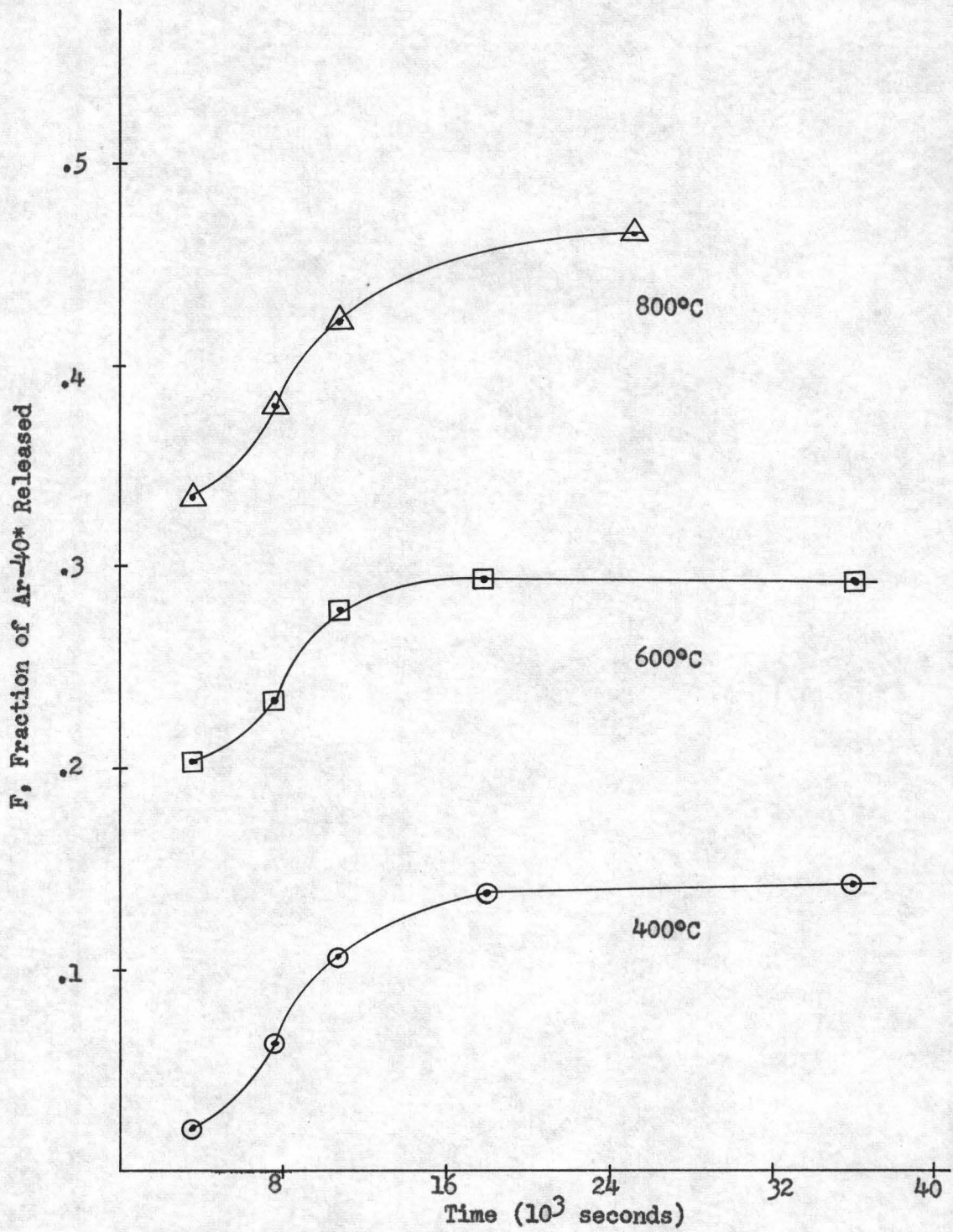


FIGURE 3 - Plot of Fraction Released vs Time for Palolo at 400°, 600° and 800°C

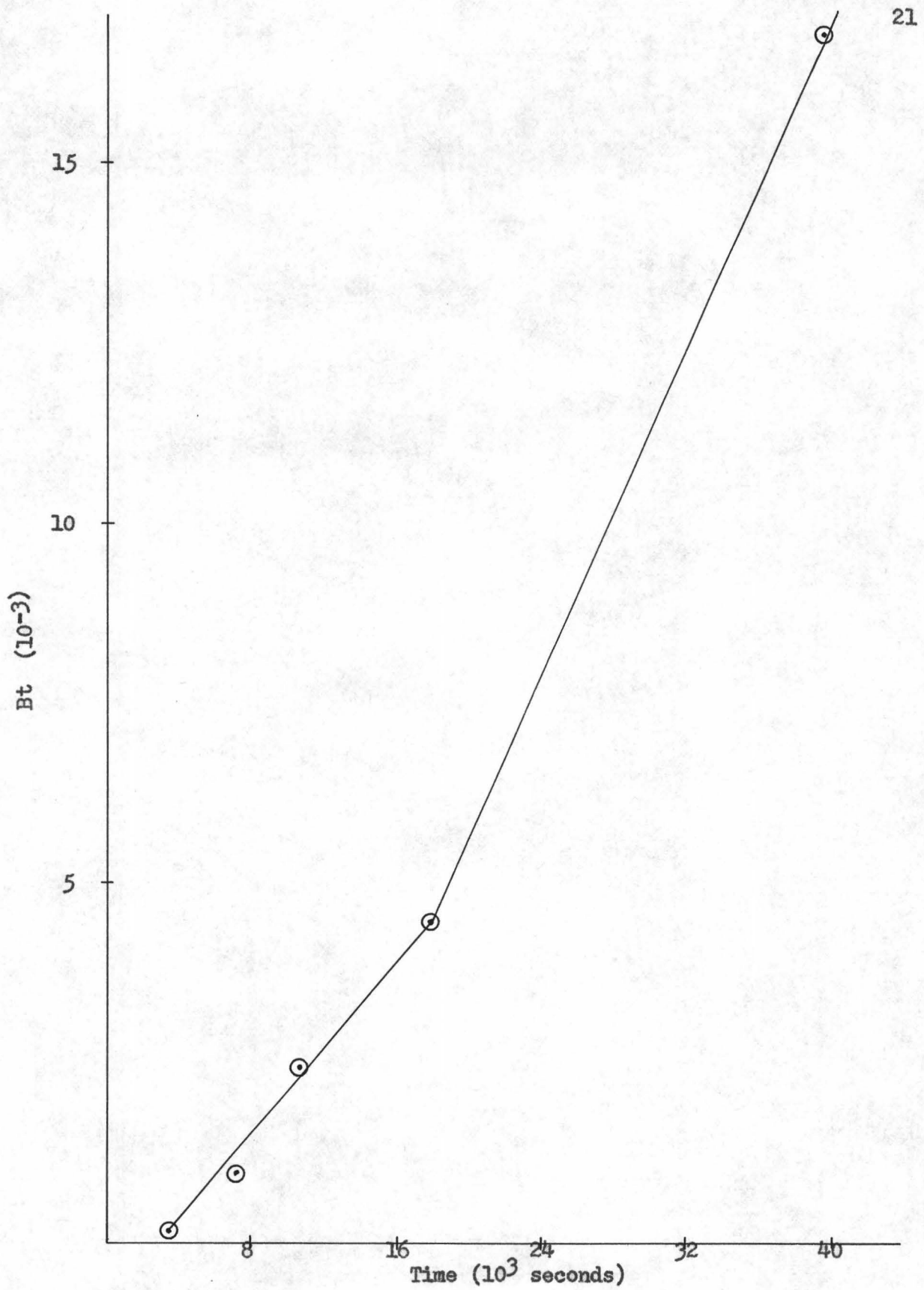


FIGURE 4 - Plot of Bt vs Time for HK 12 at 400°C

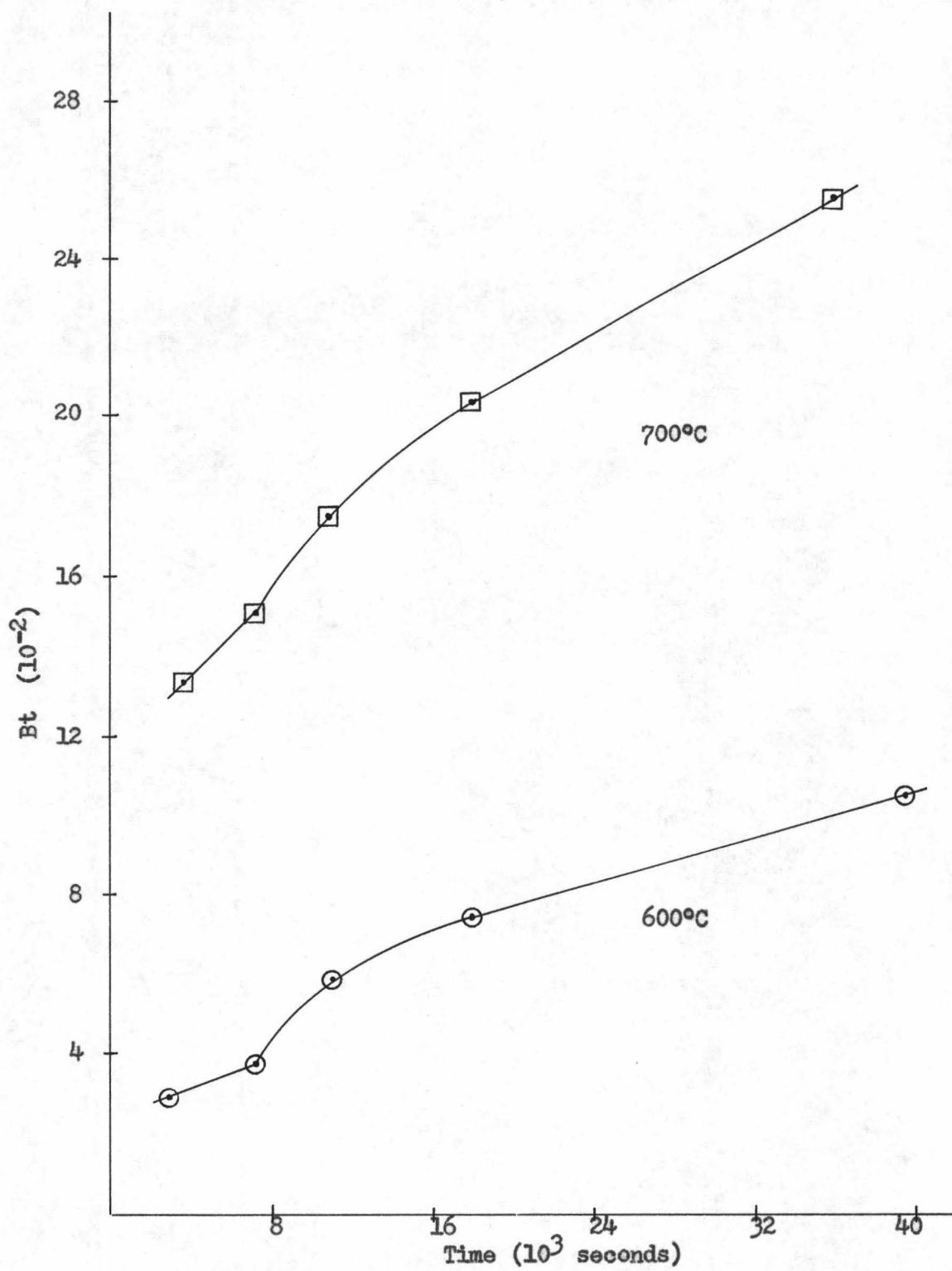


FIGURE 5 - Plot of Bt vs Time for HK 121 at 600° and 700°C

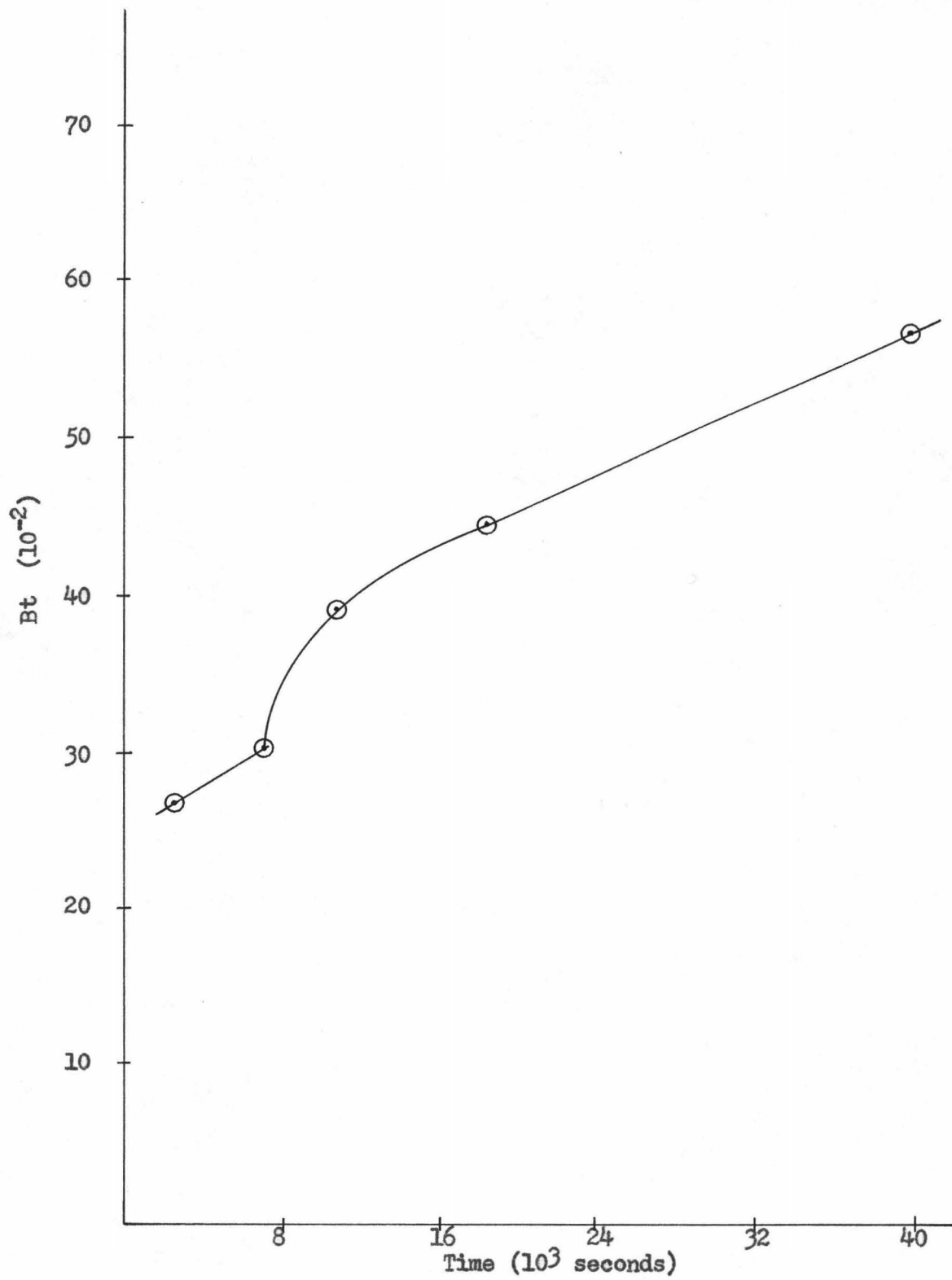


FIGURE 6 - Plot of Bt vs Time for HK 121 at 800°C

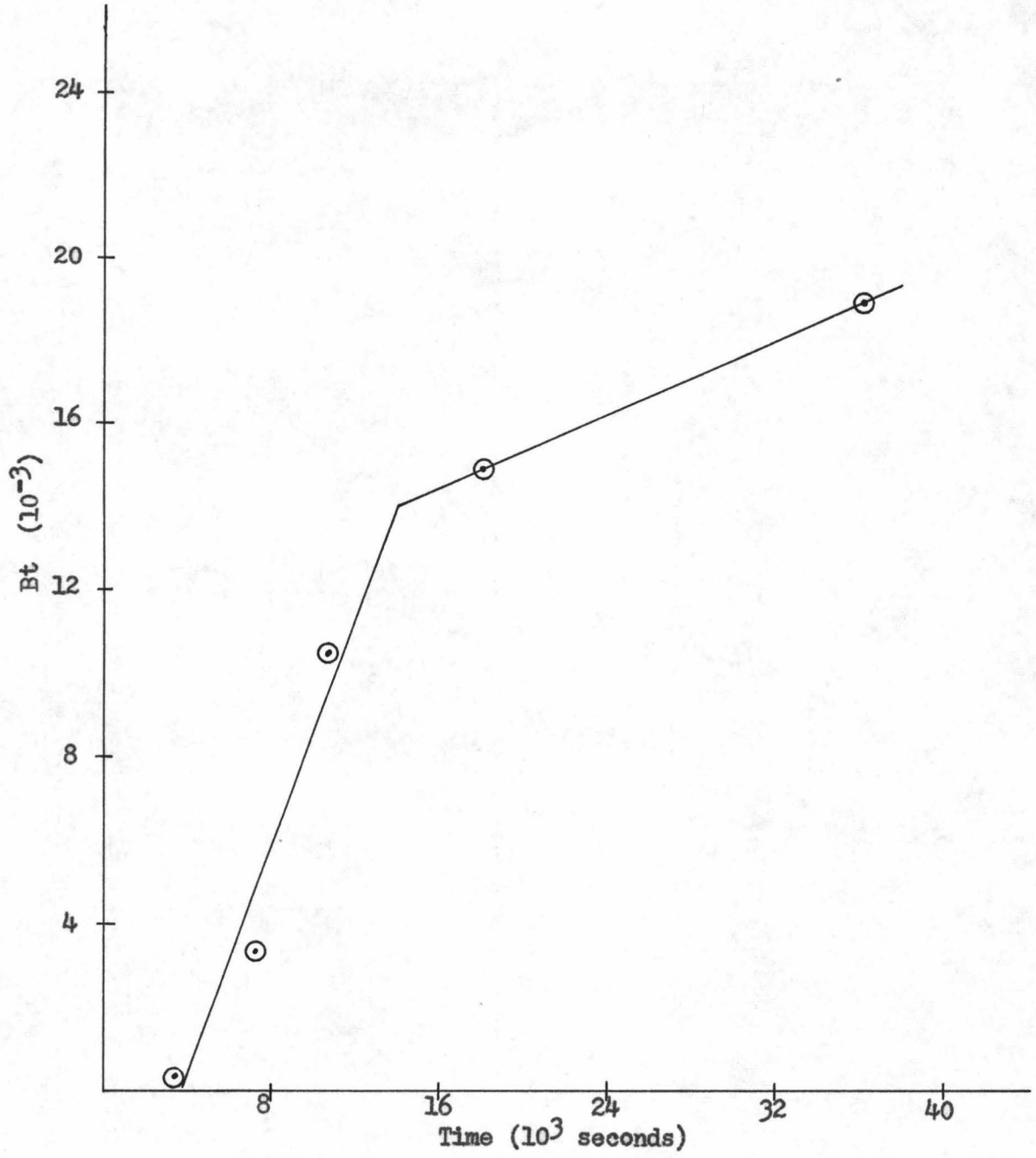


FIGURE 7 - Plot of Bt vs Time for Palolo at 400°C

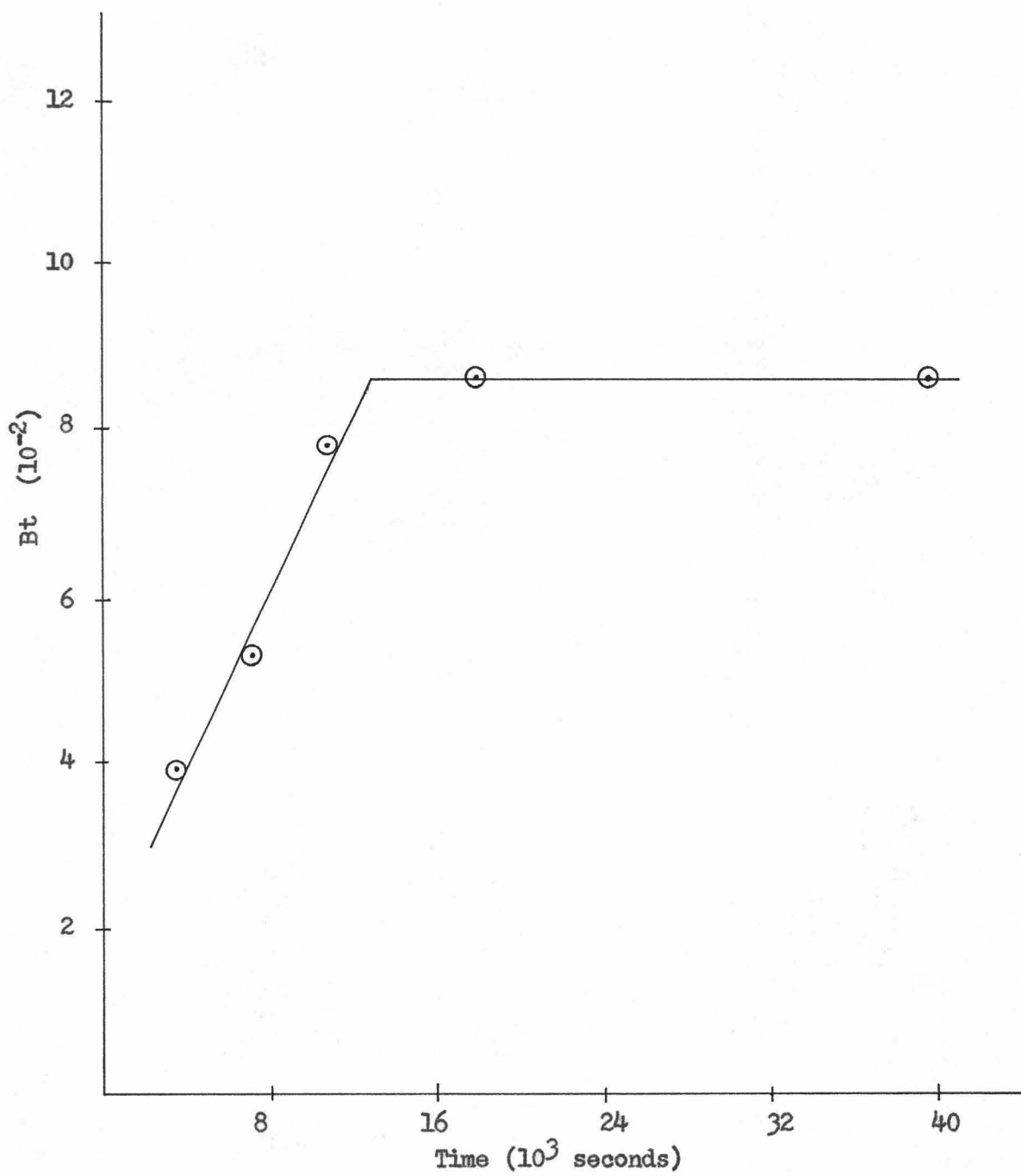


FIGURE 8 - Plot of Bt vs Time for Palolo at 600°C

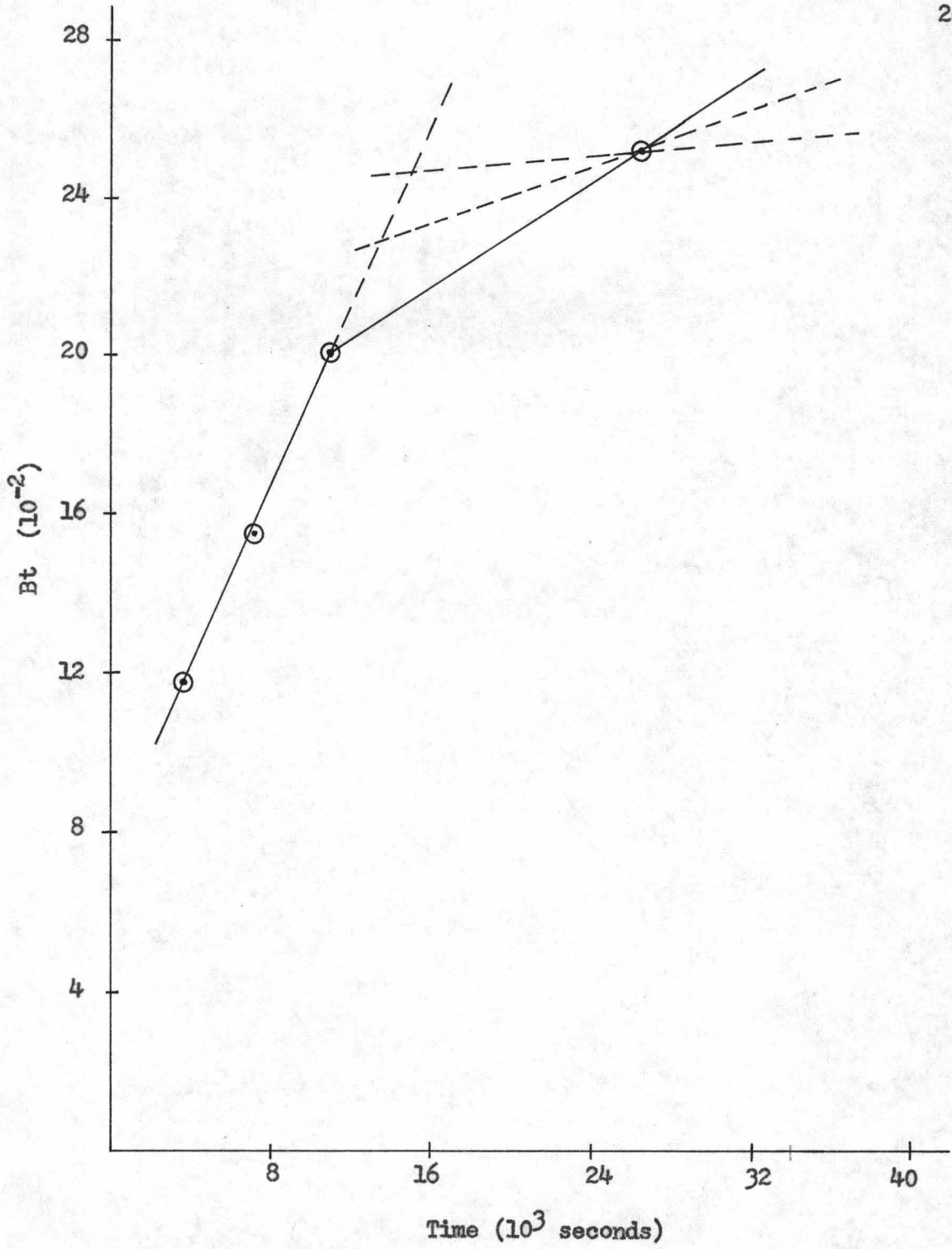


FIGURE 9 - Plot of Bt vs Time for Palolo at 800°C

temperature. When the amount of Ar-40* lost per unit time began to decrease, it appeared as a plateau on the F vs. t plots. At this stage, the Ar-40* was probably being lost by volume diffusion. All of the F vs. t plots indicate that the transition from non-volume diffusion is gradual. This is to be expected with any such natural situation where there is no sharp differentiation between diffusion from "near surface" or "volume" sites.

Figures 4 to 9, plots of Bt vs. t, were also made from the data in Tables 1 and 2. If volume diffusion were the sole type of mass transport, then these graphs would be straight lines. However, in the case of natural rock samples such as the ones used in this study, this is not to be expected. Figure 4, of HK 121 heated at 400°C, indicates that Ar-40* was probably lost in two different ways. The first segment is believed to be due to non-volume diffusion because Figure 2 shows a rapid initial Ar-40* loss characteristic of non-volume diffusion. Figures 5 and 6 of HK 121 are similar, indicating as in Figure 2, initial non-volume diffusion followed by a transition stage to volume diffusion.

Figures 7 and 8 of the Palolo sample also indicate two types of diffusion, the first probably non-volume diffusion and the second, volume diffusion. The dotted lines were drawn in Figure 9 because there was not enough data to establish exactly where the second segment lies⁽²³⁾. As can be seen from Figures 7 and 8, volume diffusion began somewhere between the third and fifth hours of heating and a data point taken after a longer heating period (e.g., 11 hours) would be necessary to show where the line actually is located. Judging from Figures 7 and 8, one of the two dotted lines

temperatures, when the amount of A-400 was just the same
to decrease, it appeared as a plateau on the 3 vs. 4 plot. All
this stage, the A-400 was probably being lost by volume diffusion.
All of the 3 vs. 4 plots indicate that the transition from non-
volume diffusion to gradual is gradual. This is to be expected with any such
actual situation where there is no sharp differentiation between
diffusion from "near surface" or "volume" sites.
Plots 1 and 2, plots of 3 vs. 4, were also made from the
data in Tables 1 and 2. If volume diffusion were the sole type
of mass transport, then these graphs would be straight lines.
However, in the case of natural rock samples such as the ones used
in this study, this is not to be expected. Figure 3, of Table 1
states at 500°C, indicates that A-400 was probably lost in two
different ways. The first way is to leave it to non-
volume diffusion. The second way is to leave it to non-
volume diffusion. Figures 1 and 2 of
the present study show that the transition from non-
volume diffusion to gradual is gradual. Figures 1 and 2 of
the present study, the transition from non-
volume diffusion to gradual is gradual.
Figures 1 and 2 of the present study also indicate two types
of diffusion, the first probably non-volume diffusion and the second,
volume diffusion. The dotted lines were drawn in Figure 3 because
there was not enough data to establish exactly how the second
segment (B) is to be drawn. As can be seen from Figures 1 and 2, volume
diffusion was somewhere between the third and fifth power of
distance and a half point case after a longer heating period (e.g.,
15 hours) could be necessary to show where the line actually is
located. Looking from Figures 1 and 2, one of the two dotted lines

better approximates the volume diffusion segment than the line drawn with only the last two data points.

The quantity B is related to the diffusion coefficient by $B = \pi^2 D/a^2$. If a, the effective radius of the particle were known, D could easily be found. However, there is much uncertainty in this quantity, therefore D/a^2 is usually used. From Bt found above, B was calculated:

$$\frac{Bt}{t} = \frac{D}{a^2}$$

where t is the time interval over which the sample was heated. The quantities calculated are presented in Tables 3 and 4 and in Figures 10 and 11.

The curves from 600°, 700°, and 800°C in Figure 10 are similar in shape and indicate a rapid loss with the characteristically high D/a^2 rates of non-volume diffusion when the sample was first heated at a higher temperature. After this easily-lost material was released, volume diffusion became apparent.

On the other hand, the curve for 400°C began with a low D/a^2 rate which rose as heating was continued, then fell and began rising again, this time more slowly. The unusual shape of this curve could result if one or more of the data points were wrong. However, this initial rise in the rate of D/a^2 , a subsequent fall, then a gradual rise also appears in Figure 11 for the Palolo sample. Both curves are for the first temperature setting. Therefore it is believed that there might be a logical explanation for this phenomena. As explained above, it is believed that non-volume diffusion takes place during the first few periods at all

TYPE-B CASE

EXPERIMENTAL

Figure 10 and 11. The curves from 6000, 7000, and 8000 in Figure 10 are similar to those in Figure 9 and indicate a rapid loss with the characteristic high rate of non-volume diffusion when the sample was first heated at a higher temperature. For this sample, the initial rate was relatively low, and the curves for 4000 began with a low rate, which rose as heating was continued. When the fall and began rising again, this was more slowly. The general shape of this curve could result if one or more of the data points were wrong. However, the initial rise at the rate of 100, a spread of 100, and a general rise also appears in Figure 11 for the other sample. Both curves are for the first temperature cooling. Therefore, it is believed that there might be a logical explanation for the phenomena. As explained above, it is believed that the volume diffusion takes place during the first two periods of all

$$\frac{dV}{dt} = \frac{dV}{dt}$$

Figure 10 and 11. The curves from 6000, 7000, and 8000 in Figure 10 are similar to those in Figure 9 and indicate a rapid loss with the characteristic high rate of non-volume diffusion when the sample was first heated at a higher temperature. For this sample, the initial rate was relatively low, and the curves for 4000 began with a low rate, which rose as heating was continued. When the fall and began rising again, this was more slowly. The general shape of this curve could result if one or more of the data points were wrong. However, the initial rise at the rate of 100, a spread of 100, and a general rise also appears in Figure 11 for the other sample. Both curves are for the first temperature cooling. Therefore, it is believed that there might be a logical explanation for the phenomena. As explained above, it is believed that the volume diffusion takes place during the first two periods of all

Table 3

Data for Diffusion Curves for HK 121

Temperature (°C)	Cumulative time (hours)	D/a^2	Log D/a^2
400	1	5.90×10^{-9}	-8.229
	2	1.37×10^{-8}	-7.863
	3	2.29×10^{-8}	-7.640
	5	1.25×10^{-8}	-7.904
	11	4.29×10^{-8}	-7.367
600	1	8.64×10^{-7}	-6.063
	2	5.28×10^{-7}	-6.277
	3	5.51×10^{-7}	-6.259
	5	2.08×10^{-7}	-6.682
	11	2.66×10^{-7}	-6.575
700	1	3.76×10^{-6}	-5.425
	2	2.11×10^{-6}	-5.675
	3	1.64×10^{-6}	-5.785
	5	5.74×10^{-7}	-6.241
	11	6.78×10^{-7}	-6.169
800	1	7.80×10^{-6}	-5.108
	2	4.27×10^{-6}	-5.370
	3	3.68×10^{-6}	-5.434
	5	1.25×10^{-6}	-5.903
	11	1.45×10^{-6}	-5.838

(Table)

Table for Diffusion Coefficients for H₂

Temperature (°C)	Diffusion Coefficient (cm ² /sec)	Relative Error (%)	Notes
100	1.00 x 10 ⁻⁵	± 2.0	
110	1.10 x 10 ⁻⁵	± 2.0	
120	1.20 x 10 ⁻⁵	± 2.0	
130	1.30 x 10 ⁻⁵	± 2.0	
140	1.40 x 10 ⁻⁵	± 2.0	
150	1.50 x 10 ⁻⁵	± 2.0	
160	1.60 x 10 ⁻⁵	± 2.0	
170	1.70 x 10 ⁻⁵	± 2.0	
180	1.80 x 10 ⁻⁵	± 2.0	
190	1.90 x 10 ⁻⁵	± 2.0	
200	2.00 x 10 ⁻⁵	± 2.0	
210	2.10 x 10 ⁻⁵	± 2.0	
220	2.20 x 10 ⁻⁵	± 2.0	
230	2.30 x 10 ⁻⁵	± 2.0	
240	2.40 x 10 ⁻⁵	± 2.0	
250	2.50 x 10 ⁻⁵	± 2.0	
260	2.60 x 10 ⁻⁵	± 2.0	
270	2.70 x 10 ⁻⁵	± 2.0	
280	2.80 x 10 ⁻⁵	± 2.0	
290	2.90 x 10 ⁻⁵	± 2.0	
300	3.00 x 10 ⁻⁵	± 2.0	

EAGLE-A
 TYPE-ERASE
 25% COTTON FIBER

Table 4

Data for Diffusion Curves for Palolo

Temperature (°C)	Cumulative time (hours)	D/a ²	Log D/a ²
400	1	1.02 x 10 ⁻⁸	-7.992
	2	4.72 x 10 ⁻⁸	-7.326
	3	9.82 x 10 ⁻⁸	-7.008
	7	6.63 x 10 ⁻⁸	-7.178
600	1	1.11 x 10 ⁻⁶	-5.956
	2	7.47 x 10 ⁻⁷	-6.126
	3	7.34 x 10 ⁻⁷	-6.134
	7	3.48 x 10 ⁻⁷	-6.458
800	1	3.31 x 10 ⁻⁶	-5.480
	2	2.18 x 10 ⁻⁶	-5.661
	3	1.88 x 10 ⁻⁶	-5.727
	7	1.01 x 10 ⁻⁶	-5.996

LEAGUE TYPE-BRASE SOL-GOLD-FIBRE

Table 4

Tests for Diffusion Coefficients for Fatigue

Log Life	Stress	Diffusion Time (hr)	Temperature (°C)
1.00	1.00 x 10 ⁷	1	300
1.10	1.00 x 10 ⁷	2	300
1.20	1.00 x 10 ⁷	3	300
1.30	1.00 x 10 ⁷	4	300
1.40	1.00 x 10 ⁷	5	300
1.50	1.00 x 10 ⁷	6	300
1.60	1.00 x 10 ⁷	7	300
1.70	1.00 x 10 ⁷	8	300
1.80	1.00 x 10 ⁷	9	300
1.90	1.00 x 10 ⁷	10	300
2.00	1.00 x 10 ⁷	11	300
2.10	1.00 x 10 ⁷	12	300
2.20	1.00 x 10 ⁷	13	300
2.30	1.00 x 10 ⁷	14	300
2.40	1.00 x 10 ⁷	15	300
2.50	1.00 x 10 ⁷	16	300
2.60	1.00 x 10 ⁷	17	300
2.70	1.00 x 10 ⁷	18	300
2.80	1.00 x 10 ⁷	19	300
2.90	1.00 x 10 ⁷	20	300

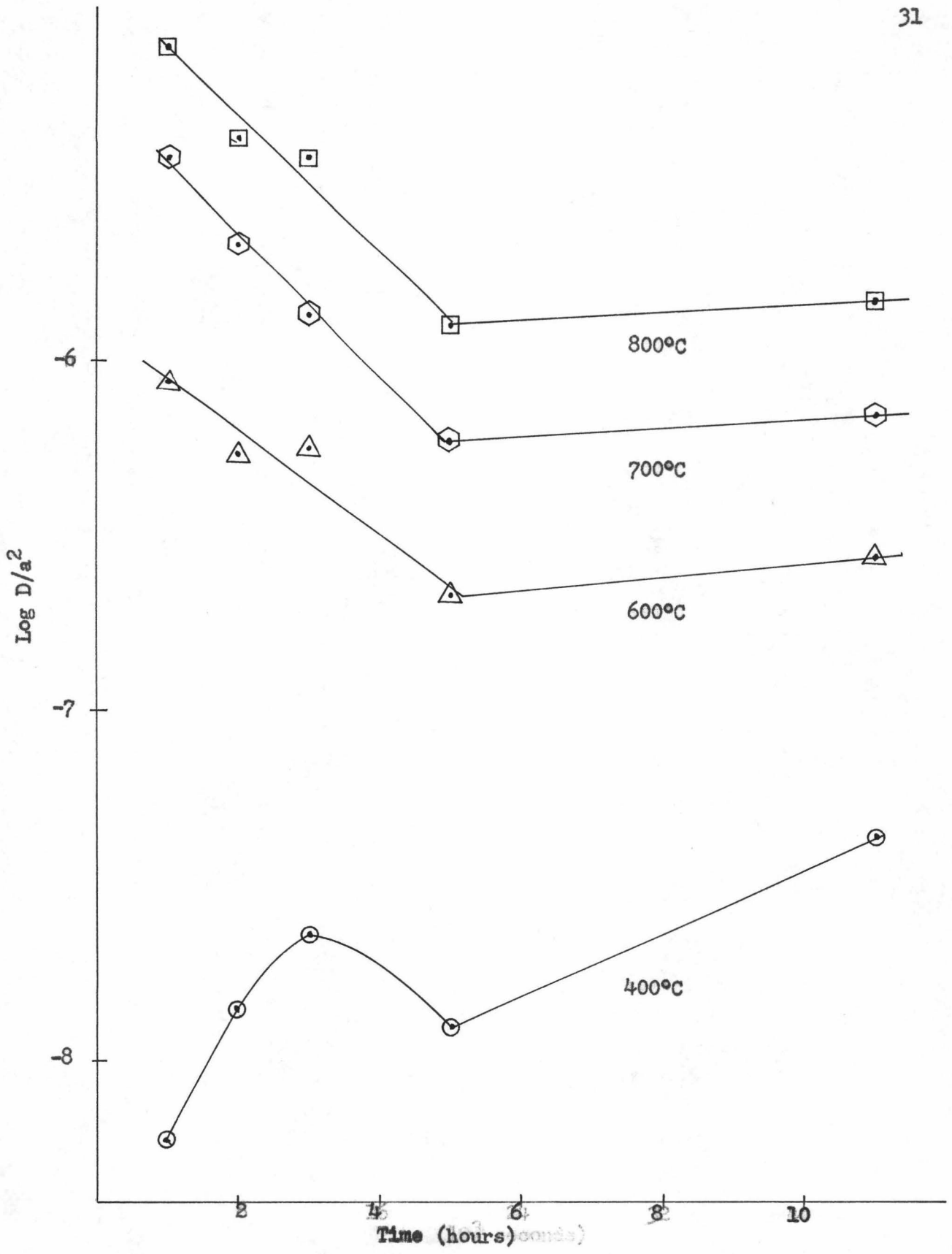


FIGURE 10 - Plot of $\text{Log } D/a^2$ vs Time for HK 121 at 400°, 600°, 700° and 800°C

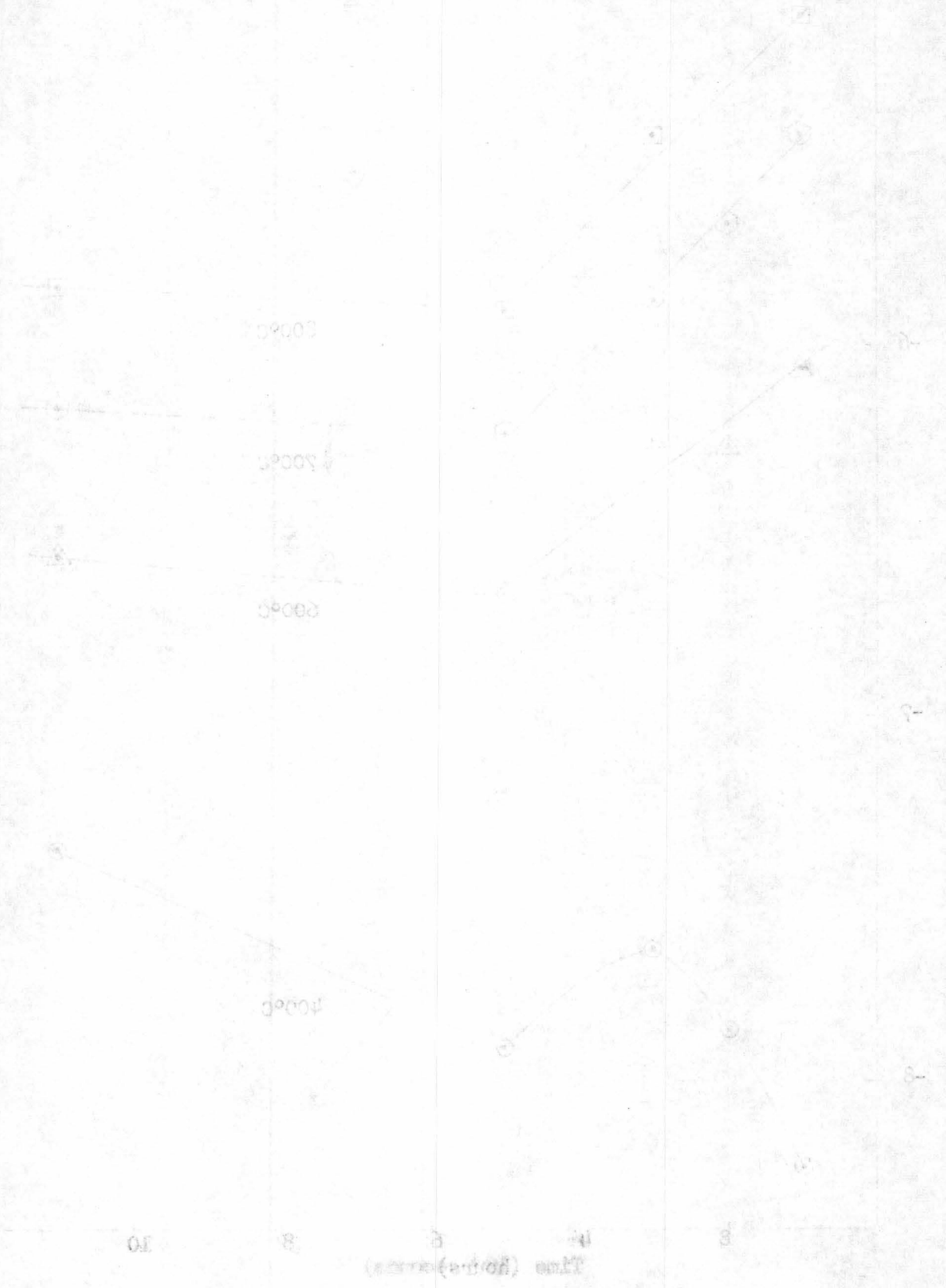


FIGURE 10 - Plot of $\log D/S$ vs time for W JMI at 800°, 700°, and 600°C

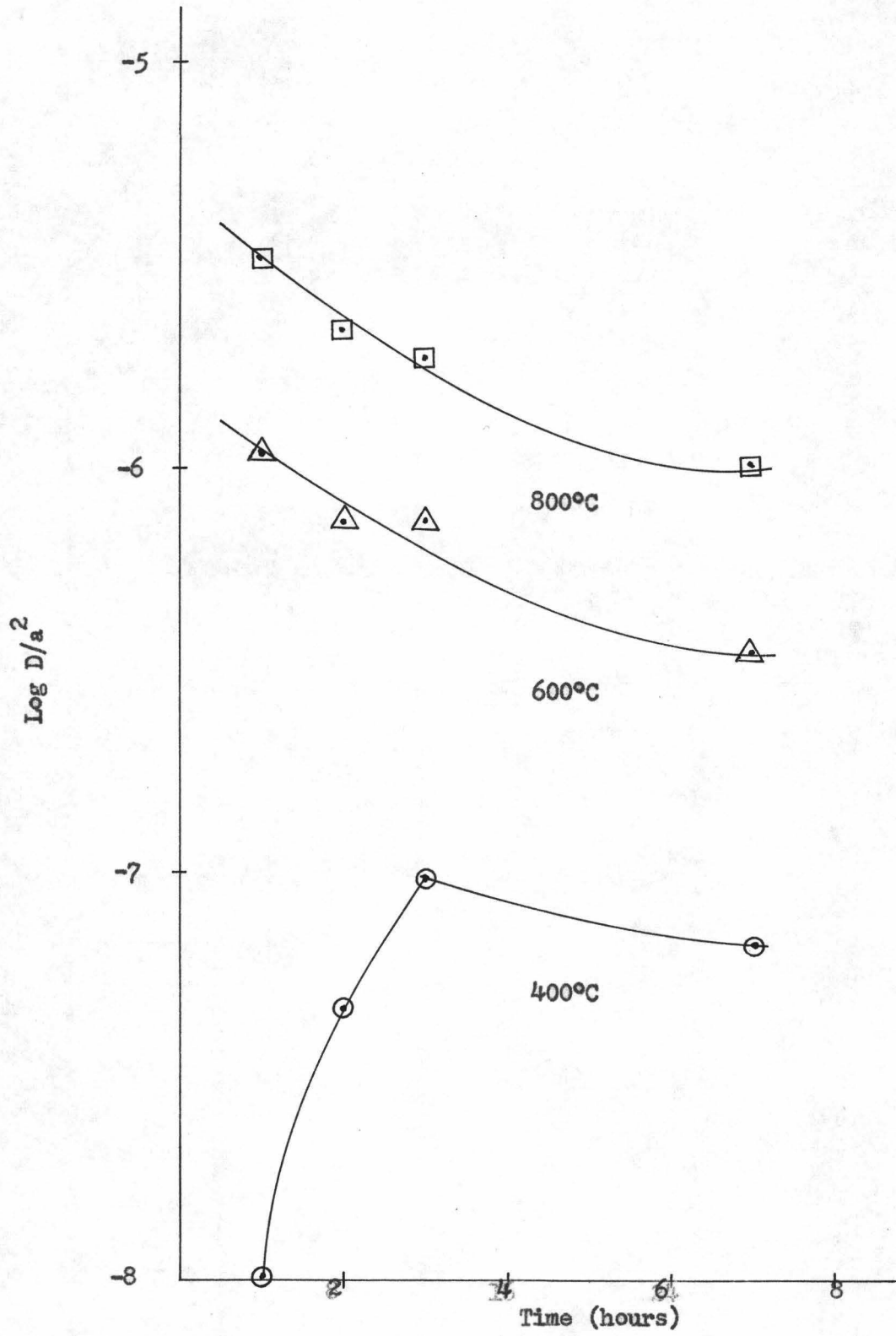


FIGURE 11 - Plot of $\text{Log } D/a^2$ vs Time for Palolo at 400°, 600° and 800°C

temperatures. Non-volume diffusion includes diffusion from areas in or at surfaces and surface irregularities. Now, diffusion from these cracks or surface irregularities requires that enough energy be available for the diffusion process as well as the desorption process from the surface. Since surface energies can be quite large, the low rates of diffusion which appear in the plots when the sample is first heated are not at all unusual⁽²³⁾. After the Ar-40* trapped on the surfaces is released, the Ar-40* not bound by adsorption can escape with higher D/a^2 rates. Then, after this more rapid non-volume diffusion has taken place, the remaining Ar-40* can come only from volume sites, a process which proceeds at a slower D/a^2 rate. In support of this argument that surface-adsorbed material was being released, it should be noted that only the more rapid, characteristically high D/a^2 rates of non-volume diffusion appear during the first few hours of heating at subsequent temperature increments. Thus the curves for 400°C in Figures 10 and 11 are not as unusual as they might first appear.

Using the Arrhenius equation,

$$D = D_0 \exp(-E/RT)$$

the activation energy, E , for volume diffusion of Ar-40* can be found from $\text{Log } D/a^2$ vs. $1000/T^\circ\text{K}$ plots. Therefore the $\text{Log } D/a^2$ values for the volume diffusion segments of Figure 10 were plotted in Figure 12. The activation energy calculated for the volume diffusion from HK 121 was 15 kcal/mole.

A similar scheme was followed for the Palolo sample. Figure 11, which corresponds to Figure 10 for HK 121, shows similar results. The curve for 400°C has been explained above. The curves for 600°

The results obtained from the present study are shown in Figure 1. The curves for 600°C
 which corresponds to Figure 10 for the IAI, shows similar results. The curve for 600°C
 which corresponds to Figure 10 for the IAI, shows similar results. A similar behavior was
 observed for the IAI samples, Figure 11. The activation energy calculated for the volume
 values from the volume fraction curves of Figure 10 were plotted
 found from the IAI vs. 1000/T plots. Therefore the log 10 of
 the activation energy, E, for volume fraction of IAI can be

$$E = 1.8 \times 10^4 \text{ cal/mole}$$
 which is the Arrhenius equation.
 as shown in Figure 10 and 11 are
 during the first two hours of heating at subsequent temperatures
 observed. Finally the values of non-volume fraction
 was determined. It should be noted that only the more
 1000/T. In support of this statement that surface-adsorbed
 can come only from volume fraction, a process which proceeds at a
 rapid non-volume fraction has taken place, the remaining
 also has been with IAI. Then, after this
 process on the surface is released, the
 sample is first heated at a
 large, the rate of diffusion is
 process from the surface, since surface
 be available for the diffusion process.
 these cracks or surface irregularities that
 to or at surface and surface irregularities,
 temperature. Non-volume fraction

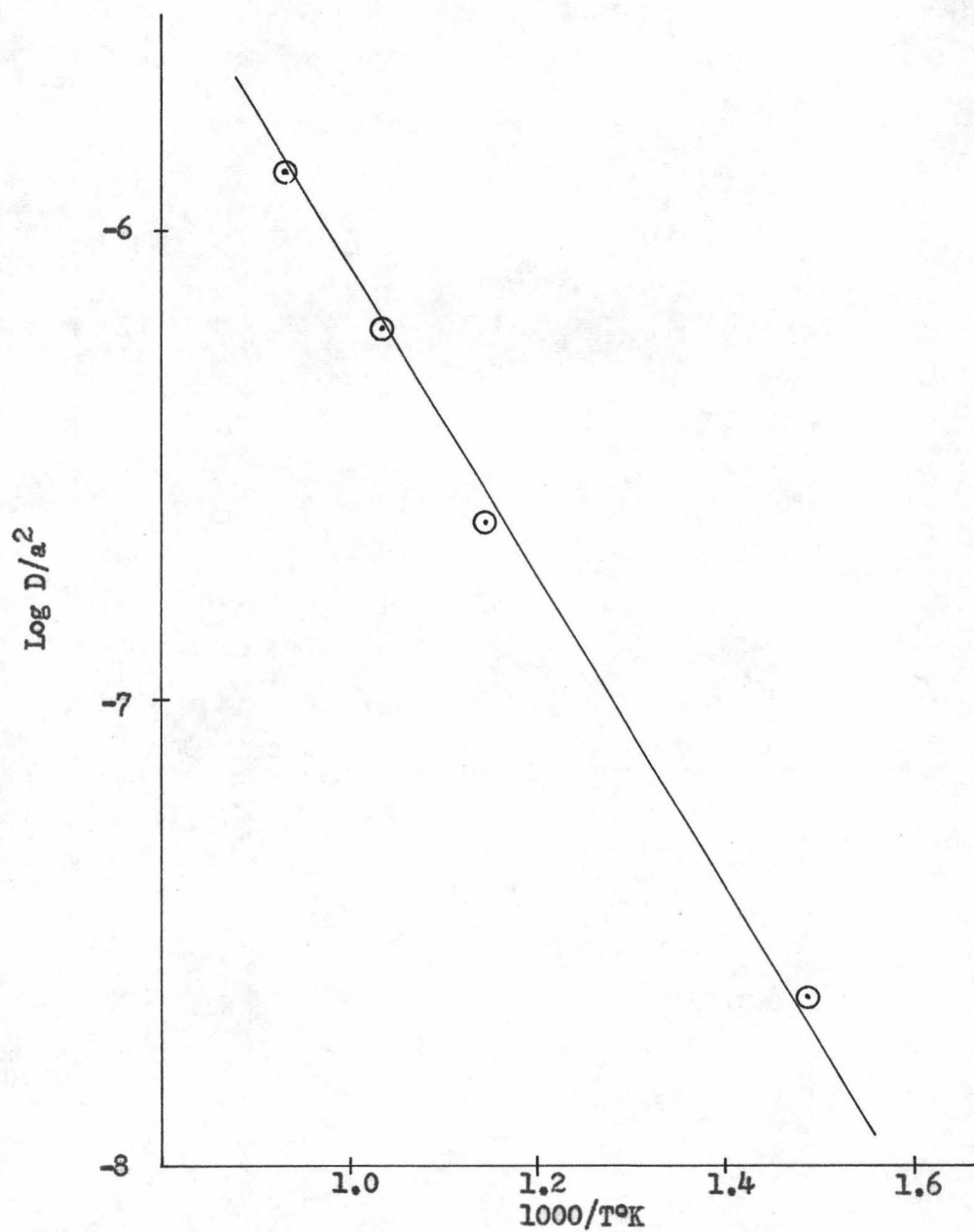


FIGURE 12 - Plot of $\text{Log } D/a^2$ vs $1000/T^{\circ}\text{K}$ for HK 121

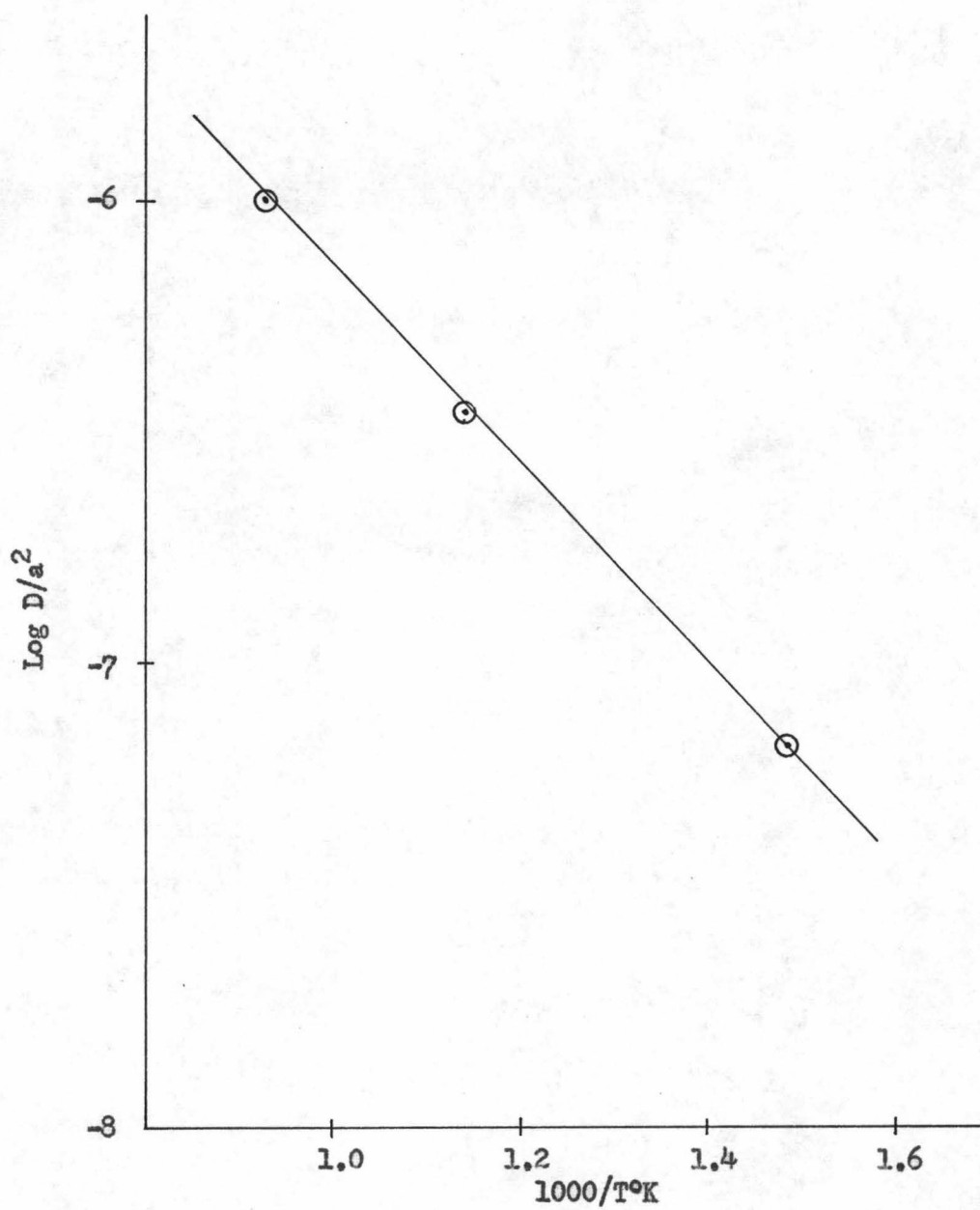


FIGURE 13 - Plot of $\text{Log } D/a^2$ vs $1000/T^{\circ}\text{K}$ for Palolo

and 800°C are similar to the higher temperature curves for HK 121 in Figure 10, in that they show a high loss of Ar-40* during initial heating, with volume diffusion setting in with lower D/a^2 rates as heating was continued. A Log D/a^2 vs. $1000/T^\circ K$ plots was made for the Palolo sample (Figure 13) and the resulting single line indicated that there was only one type of volume diffusion taking place, with an activation energy of 9.8 kcal/mole.

The data for the potassium-aluminum-silicate (KAS) in Barnes' work⁽²⁾ was treated in a similar manner. Table 5 for KAS is comparable to Tables 3 and 4 for HK 121 and Palolo, respectively. Figure 14 was drawn from this data. As can be seen, the curves are similar in shape to those of HK 121 and Palolo (Figures 10 and 11, respectively). There is no curve which is comparable in shape to that of the 400°C curves in Figures 10 and 11 because the KAS was not heated for several time periods at the initial temperature. Such curves, as pointed out above, would appear only with the very first heating periods. The curves which are plotted show the decrease in the D/a^2 values with a tendency to level off as volume diffusion begins. As can be seen, the curve for 600°C reaches a plateau at about $4\frac{1}{2}$ hours. Thus, although the sample was not heated for longer periods of time at 700° and 800°C, it can probably be assumed that the D/a^2 value would become constant with time after approximately four hours. The general shapes of the curves indicate that this probably is a valid assumption.

What appears to be unusual about the plots in Figure 14 is that the 700° and 800°C curves appear to have the same D/a^2 for volume diffusion. Thus, when Log D/a^2 vs. $1000/T^\circ K$ is plotted for

and 800°C are similar to the higher temperature curves for 100°C
in Figure 10, in that they show a sharp loss of ΔV_s volume fraction
beginning with volume fraction cooling in with lower ΔV_s values as
heating was continued. At 100°C vs. 1000°C ΔV_s data was made
for the failed sample (Figure 10) and the resulting curves are
indicated that there was only one type of volume fraction change
place, with an activation energy of 2.8 kcal/mole.
The data for the potassium-sulfate-sulfate (KPS) in
Figure 10 was treated in the same manner. Table 2 for KPS
is comparable to Figure 10 and 11 and 12, respectively.
Figure 10 has been plotted in Figure 10. As can be seen, the curves
are similar to those of Figure 10 and 11, respectively. There is no
appreciable change in ΔV_s values which is comparable in shape
to that of the 100°C curve in Figure 10 and 11 because the KPS
was not heated for several time periods at the initial temperature.
Each curve, as pointed out above, would appear only with the very
first heating periods. The curves which are plotted show the
decrease in the ΔV_s values with a tendency to level off as volume
fraction heating. As can be seen, the curve for 800°C reaches a
plateau at about 40 hours. Thus, during the sample was not heated
for longer periods of time at 700°C and 800°C, it can probably be
assumed that the ΔV_s value would become constant with time after
approximately four hours. The general shape of the curves indicate
that this probably is a valid assumption.
It appears to be unusual that the plots in Figure 10
is that the 700°C and 800°C curves appear to have the same ΔV_s for
volume fraction. Thus, when the ΔV_s vs. 1000°C is plotted for

Table 5

Data for Diffusion Curves for KAS

Temperature (°C)	Cumulative time (hours)	D/a^2	$\text{Log } D/a^2$
600	1	2.45×10^{-7}	-6.61
	2	1.60×10^{-7}	-6.79
	3	1.47×10^{-7}	-6.83
	$4\frac{1}{2}$	1.26×10^{-7}	-6.90
	$5\frac{1}{2}$	1.26×10^{-7}	-6.90
700	1	8.08×10^{-7}	-6.09
	2	4.38×10^{-7}	-6.36
	3	3.05×10^{-7}	-6.52
	4	2.34×10^{-7}	-6.63
800	1	9.51×10^{-7}	-6.02
	2	4.77×10^{-7}	-6.32
	3	3.20×10^{-7}	-6.49
	4	2.34×10^{-7}	-6.63

Data for 1954-55 (1955)

Year	Temperature (°C)	...
1954	100	...
1955	100	...
1956	100	...
1957	100	...
1958	100	...
1959	100	...
1960	100	...
1961	100	...
1962	100	...
1963	100	...
1964	100	...
1965	100	...
1966	100	...
1967	100	...
1968	100	...
1969	100	...
1970	100	...
1971	100	...
1972	100	...
1973	100	...
1974	100	...
1975	100	...
1976	100	...
1977	100	...
1978	100	...
1979	100	...
1980	100	...
1981	100	...
1982	100	...
1983	100	...
1984	100	...
1985	100	...
1986	100	...
1987	100	...
1988	100	...
1989	100	...
1990	100	...
1991	100	...
1992	100	...
1993	100	...
1994	100	...
1995	100	...
1996	100	...
1997	100	...
1998	100	...
1999	100	...
2000	100	...

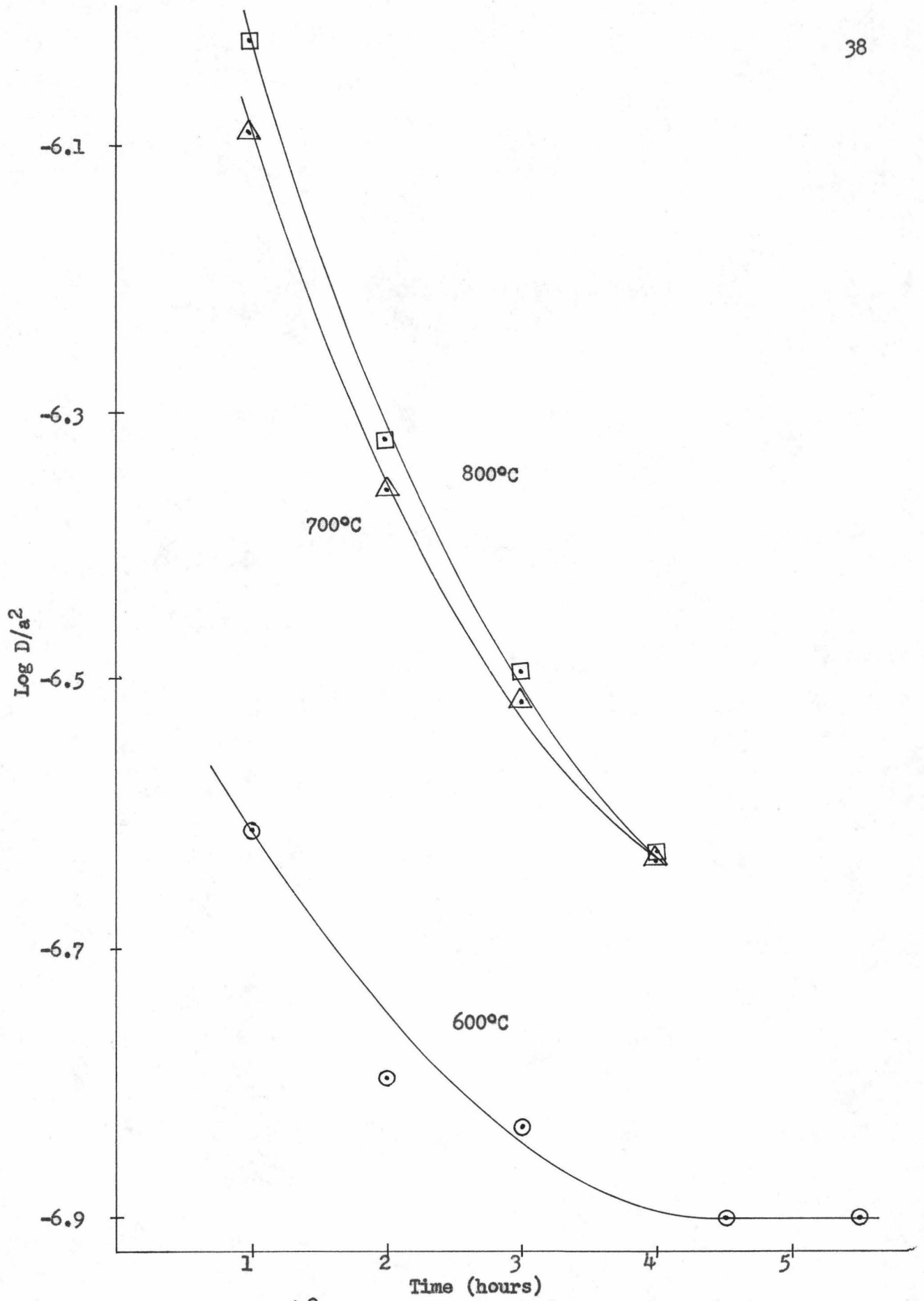


FIGURE 14 - Plot of Log D/a² vs Time for KAS at 600°, 700° and 800°C

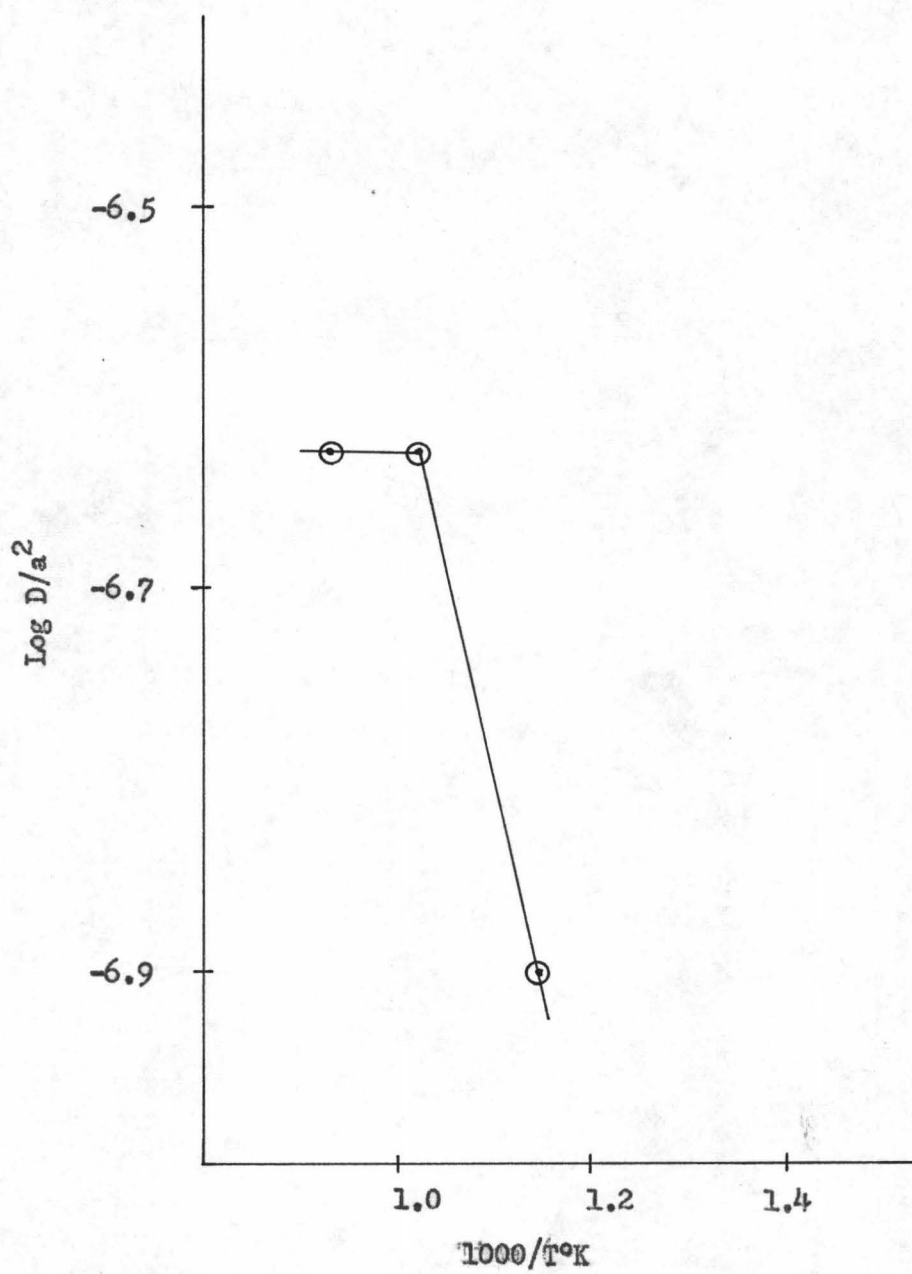


FIGURE 15 - Plot of $\text{Log } D/a^2$ vs $1000/T^{\circ}\text{K}$ for KAS

KAS, there are two activation energies for volume diffusion.

(See Figure 15) The activation energy of 0.04 kcal/mole is very small and probably results during a change of phase or other internal transitions within the glass between 700° and 800°C, as suggested by Barnes⁽²⁾. X-ray diffraction powder photographs of the KAS were made before and after the heating process. The photograph of the material before heating showed no diffraction lines at all, indicating a completely amorphous structure. The photograph taken after the heating had a definite diffraction pattern corresponding to that of crystalline leucite.

Assuming that the activation energies for volume diffusion also apply at lower temperatures, then F, the fraction of argon lost at temperatures usually used for bakeout can be calculated. The data are summarized in Table 6 and plotted as Figure 16. As can be seen from the plot, the fraction of argon lost increases rapidly with increase in bakeout temperatures. If KAS were baked out at 400°C for 12 hours, it would lose about 23% of its total Ar-39 content, while a Palolo sample would lose about 17% of its total Ar-40* content and HK 121 about 10%.

The volume diffusion proceeds more rapidly in Palolo than in HK 121. This is not unusual because the rocks are composed of different minerals probably with different grain sizes. The Palolo rock is made up of about 29% albite, 20% anorthite, 16% hypersthene and 15% diopside, while HK 121 has about 38% albite, 26% orthoclase and 16% quartz⁽¹⁵⁾.

If a natural sample were mixed with the KAS and baked out at a temperature above 150°C, then it would lose more of its contaminating

...there are two distinct energies for volume diffusion.

(See Figure 15) The activation energy of 0.6 eV corresponds to the

small and probably results from a change of phase or other internal

transition which the glass between 700° and 800°, as suggested

by Figure 15. A low diffusion powder procedure of the glass

were made before and after the heating process. The procedure

of the material before heating showed no diffusion lines at all,

indicating a highly ordered structure. The procedure taken

at the present time has a definite structure, but corresponding

to that of the original state.

Assuming that the energy of activation for volume diffusion

also applies to inter-composition, then the fraction of oxygen

lost at temperatures usually used for deaeration can be calculated.

The data are summarized in Table 2 and plotted in Figure 16. As

can be seen from the plot, the fraction of oxygen lost increases

rapidly with increase in deaeration temperature. It has been found

that at 700°C to 715°C, it would lose about 2% of the total

oxygen content, while at 800°C the oxygen loss is about 1% of the

total oxygen content and at 900°C about 1%.

The volume diffusion process was rapid in Table 15 at

1000°C. This is not unusual, because the rocks are composed of

different minerals probably with different crystal sizes. The volume

rock is made up of about 50% alpha, 20% anorthite, 10% hypersthene

and 20% diopside, while B. 151 has about 70% alpha, 20% orthoclase

and 10% quartz (15).

If a natural sample were mixed with the B. 151 and baked out

at a temperature above 1200°C, then it would lose more of its oxygen

Table 6

Fraction of Argon Released by Volume Diffusion
at Different Temperatures During a 12-Hour Heating Period

Sample	Temperature (°C)	F, Fraction Released (10 ⁻²)
KAS	400	23.3
	300	5.13
	200	1.97
	150	1.03
	100	0.449
HK 121	400	10.4
	300	3.98
	200	0.996
	150	0.389
	100	0.117
Palolo	400	17.3
	300	9.31
	200	3.79
	150	2.05
	100	0.940

Division of transportation and traffic control
at the state capital building, Harrisburg, Pa.

Personnel, Pennsylvania State Police

Grade	Number	Rate
10.1	100	100
9.1	100	90
8.1	100	80
7.1	100	70
6.1	100	60
5.1	100	50
4.1	100	40
3.1	100	30
2.1	100	20
1.1	100	10

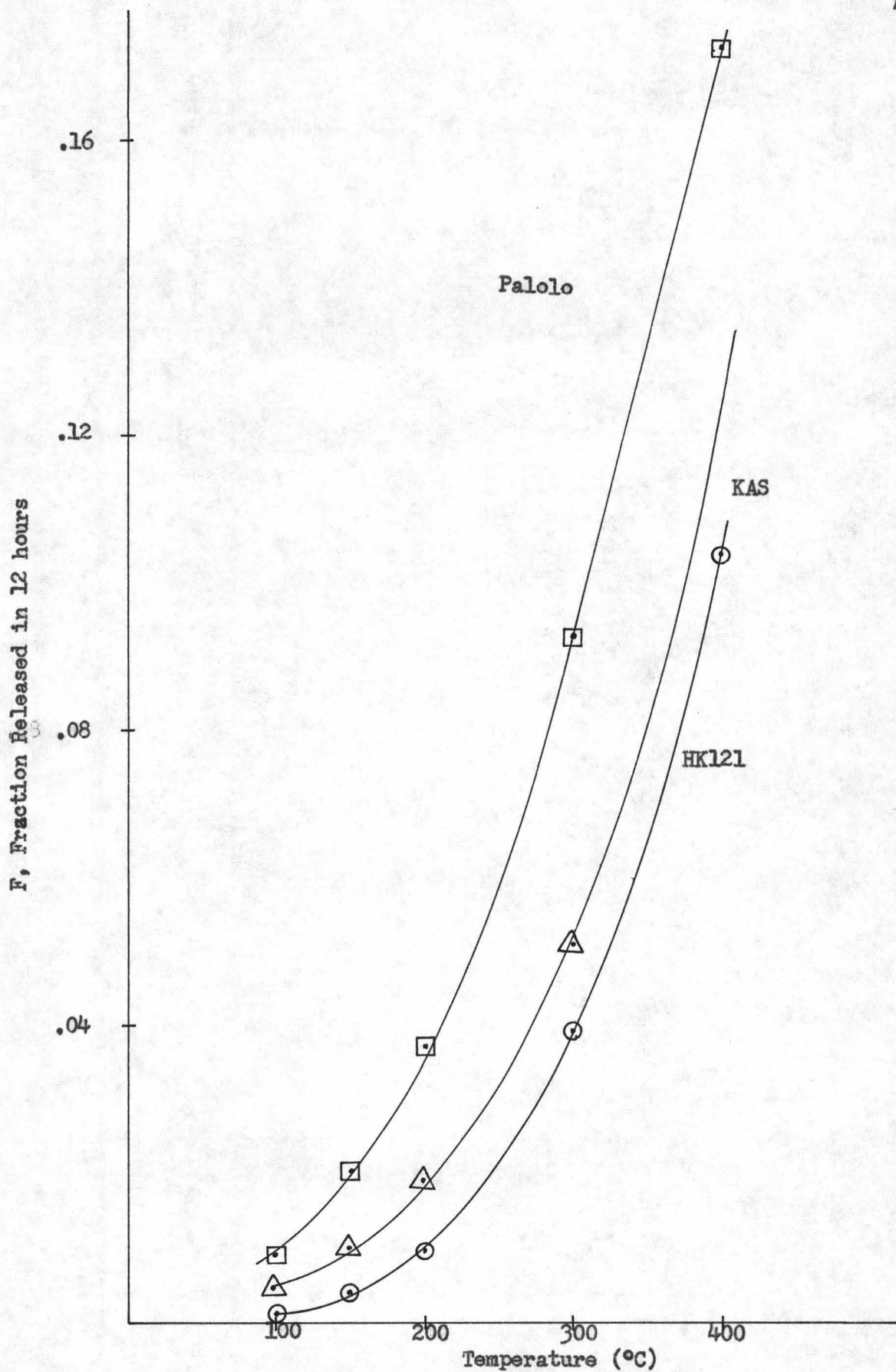


FIGURE 16 - Plot of Fraction Released in 12 hours by Volume Diffusion vs Temperature for KAS, HK 121 and Palolo

air Ar-40 and the amount of Ar-40* can be found from a plot like Figure 16. The average amount of Ar-40* lost by non-volume diffusion at each temperature during the first five hours of heating was about 10% for HK 121 and 14% for the Palolo sample. Non-volume diffusion can be expected to vary from sample to sample of even the same rock because it is diffusion from surface and surface irregularities which naturally would differ from sample to sample. Therefore with additional diffusion studies, perhaps an average value to be used in calculating the amount of Ar-40* lost due to non-volume diffusion can be found.

Although the volume diffusion loss of Ar-39 from KAS and the Ar-40* loss from HK 121 and Palolo are not the same, Naughton's proposal⁽¹⁰⁾ of using Ar-39 as the diluting isotope could still be used successfully. If additional diffusion studies were made on other Hawaiian rocks more generally representative of the types used for K-Ar dating (e.g., tholeite basalts) then perhaps general trends could be found and diffusion studies, an extremely time-consuming procedure, as shown in II.C., would not have to be carried out for each rock to be dated. This study is a first step in that direction.

Some suggestions for future work.

As stated above, additional diffusion studies should be done in order to be able to routinely apply Naughton's proposed method of using Ar-39 as a tracer isotope. If such studies are carried out, the following suggestions might be useful.

First, a larger sample should be used for diffusion studies. The samples used in this research weighed about one-half gram.

air 2-10 and the amount of 2-10* can be found from a plot like
Figure 10. The average amount of 2-10* lost by non-volume diffusion
at each temperature during the first five hours of heating was
about 10% for 2-10 and 14% for the 2-10* sample. Non-volume
diffusion can be expected to vary from sample to sample or even the
same year because of its diffusion from surface and volume trans-
ference which naturally would differ from sample to sample.
Therefore with additional diffusion studies, within an average
value to be used in calculating the amount of 2-10* lost due
to non-volume diffusion can be found.

Although the volume diffusion loss of 2-10* from 2-10 and
the 2-10* loss from 2-10 and 2-10* are not the same, the loss
of 2-10* from 2-10* is as the diffusion factors could still
be used to estimate it. If the initial diffusion studies were not
on other samples from the general representative of the type
used for 2-10* studies (e.g., 2-10* (2-10*)) then further studies
would be required and diffusion studies, or extremely time-
consuming studies, would not have to be carried
out for each new lot of data. This study is a first step in that
direction.

Some suggestions for future work
as stated above, additional diffusion studies should be
done in order to be able to sufficiently apply Hession's research
method of using 2-10* as a check isotope. If such studies are
carried out, the following suggestions might be useful.
First, a larger sample should be used for diffusion studies.
The samples used in this research which weighed about one-half gram,

Because the amount of Ar-40* which diffuses out at one time-temperature setting is usually about 1 or 2% of the total Ar-40* present in the sample, the quantities measured were in the range of 3×10^{-9} cc. If however, a rock contained about 3×10^{-7} cc/gm of Ar-40* and a two-gram sample were used for diffusion studies then the amounts measured would be about 1×10^{-8} cc, a more reasonable quantity.

The following suggestions for improvement in procedures may seem trivial to a casual reader. But a person engaged in scientific research knows that the many little problems which arise in active research can add up to big problems. With this in mind, the following suggestions are made.

Improvements should be made on the gas extraction and purification system. First, more automatic timing devices should be considered for use. A step in this direction was made by attaching a timer to the Ti getter so that it could be turned on and off automatically. Second, the time involved in each run could perhaps be shortened if a better oven were constructed for the Ti getter so that it could be brought up to operating temperature more rapidly.

Another improvement in the system would be to place a charcoal finger between valve 2 and the pumping section. For these studies, liquid nitrogen was placed around the U-tube in Section IA in order to make certain the system was as clear as possible of contaminating gases from the previous run. However, it was noted that the pressure before and after liquid nitrogen was placed around the U-tube was not very different. But when liquid nitrogen was placed on a

because the amount of (A-B) which differs out of one time-
temperature being is usually about 1 or 2% of the total (A-B)
present in the sample, the quantities measured were in the range
of 3 x 10⁻⁹ cc. However, a peak contained about 3 x 10⁻⁷ cc.
of (A-B) and a two-year sample was used for diffusion studies
from the amounts measured would be about 1 x 10⁻⁷ cc. a more

reasonable quantity.

The following suggestions for improvements in procedure

may seem trivial to a casual reader, but a person engaged in
scientific research knows that the many little problems which arise
in active research can add up to big problems. With this in mind,
the following suggestions are made.

Improvements should be made on the gas extraction and

purification steps. First, more accurate data should

be considered for use. A step in this direction was made by

using the 100 cc. rather than the 10 cc. in the

extraction. Second, the time involved in each run should be

reduced. It is better to have one run for the 10 cc. rather

than two runs for the 100 cc. run.

rapidly.

Another improvement which could be made is to use a

higher temperature for the extraction. For these studies,

liquid nitrogen was used around the 100 cc. in order

to make certain the system was as clean as possible of contaminants

from the previous run. However, it was noted that the pressure

before and after liquid nitrogen was placed on the system was

not very different. But when liquid nitrogen was placed on a

charcoal finger, the pressure in the system improved greatly. This is due to the well-known fact that charcoal is an excellent adsorbent. Thus, if a charcoal finger were placed between valve 2 and the pumps, then with liquid nitrogen on the finger, the other charcoal fingers and molecular sieve traps in IA and IB could be flamed out. Then with valve 2 closed and liquid nitrogen removed, the finger could be gently flamed in order to release the contaminants which would be quickly removed by the pumps. Another advantage of placing the finger between valve 2 and the pumps is that it would be within the bake-out area.

Finally, for fusion runs the sample in the sidearm had to be made to fall into the molybdenum crucible in the quartz chamber. Much trouble was encountered on occasion when the bulky sample packets became lodged sideways in the chamber and did not fall into the crucible. Therefore it is suggested that future workers wrap the samples in the shape of a small pyramid or cube. The pyramidal or cube shape would make it possible to manipulate the samples in the sidearms without fear that all might accidentally roll into the furnace (as might happen if the packets were in the shape of a sphere), and yet be compact enough to fall into the crucible without becoming lodged in the chamber.

characteristic of the material in the system...
This is due to the well-known fact that...
When the valve is closed, the...
the finger could be gently...
which would be...
be within the...
Finally, for...
be made to fall...
such trouble was encountered...
proceeds beyond...
the orifice...
the orifice...
or else...
the orifice...
turning...
and...
pedaling...

IV. Summary

This study has shown that Naughton's proposal⁽¹⁰⁾ for using Ar-39 in an irradiated artificial glass sample as the tracer isotope for potassium-argon dating in order to reduce air contamination and improve quantitative determinations of Ar-40* is promising. Two Hawaiian rocks, HK 121 and Palolo, were studied and their diffusion parameters found.

Non-volume diffusion was apparent during the first few hours of bakeout with volume diffusion gradually becoming the mode of mass transport. Low D/a^2 rates during the first heating periods were believed to be due to the fact that energy was needed initially for both desorption and diffusion. From the information gathered, the Ar-40* loss of HK 121 and Palolo and the Ar-39 loss of KAS for a given time with respect to temperature were plotted. Such plots could be used by future workers to determine the amounts of Ar-40* lost during the bakeout.

Additional diffusion studies on rocks more representative of those used for potassium-argon dating might indicate general trends in diffusion losses at higher bake-out temperatures. If this were so, then Naughton's proposal⁽¹⁰⁾ for using Ar-39 in artificial silicate glasses for the tracer isotope could be used routinely in future geochronological studies.

This study has shown that hydrogen's presence in the reactor core is an important factor in determining the amount of heat transfer to the primary loop. The presence of hydrogen in the core can significantly increase the heat transfer coefficient, especially at low Reynolds numbers. This is due to the fact that hydrogen has a very low viscosity and high thermal conductivity. The presence of hydrogen in the core also increases the rate of convection, which further enhances heat transfer. The results of this study indicate that the presence of hydrogen in the core is a significant factor in determining the overall heat transfer performance of the reactor. The presence of hydrogen in the core can be used to improve the efficiency of the reactor and reduce the amount of fuel required to produce a given amount of power. The presence of hydrogen in the core can also be used to reduce the temperature of the primary loop, which can help to reduce the risk of overheating and improve the safety of the reactor. The presence of hydrogen in the core can also be used to reduce the amount of radiation emitted by the reactor, which can help to reduce the risk of radiation exposure to the public. The presence of hydrogen in the core can also be used to reduce the amount of waste produced by the reactor, which can help to reduce the risk of environmental contamination. The presence of hydrogen in the core can also be used to reduce the amount of time required to shut down the reactor, which can help to reduce the risk of a nuclear accident. The presence of hydrogen in the core can also be used to reduce the amount of money required to build and operate a reactor, which can help to make nuclear power more affordable. The presence of hydrogen in the core can also be used to reduce the amount of time required to build a reactor, which can help to speed up the development of nuclear power. The presence of hydrogen in the core can also be used to reduce the amount of time required to decommission a reactor, which can help to reduce the risk of a nuclear accident. The presence of hydrogen in the core can also be used to reduce the amount of time required to clean up a nuclear accident, which can help to reduce the risk of a nuclear accident. The presence of hydrogen in the core can also be used to reduce the amount of time required to build a new reactor, which can help to speed up the development of nuclear power. The presence of hydrogen in the core can also be used to reduce the amount of time required to decommission a reactor, which can help to reduce the risk of a nuclear accident. The presence of hydrogen in the core can also be used to reduce the amount of time required to clean up a nuclear accident, which can help to reduce the risk of a nuclear accident. The presence of hydrogen in the core can also be used to reduce the amount of time required to build a new reactor, which can help to speed up the development of nuclear power.

V. References

1. Schaeffer, O. A. and J. Zahringer, ed. Potassium-Argon Dating. Springer-Verlag, New York, 1966.
2. Barnes, I. L. "An Investigation of a New Method for Potassium-Argon Age Determination," Ph.D. Thesis, University of Hawaii, 1963.
3. Cook, G. S., ed. Argon, Helium and the Rare Gases. John Wiley and Sons, New York, 1961. pp. 42-43.
4. Funkhouser, J. G. "The Determination of a Series of Ages of a Hawaiian Volcano by the Potassium-Argon Method." Ph.D. Thesis, University of Hawaii, 1966.
5. Noble, Clyde. Ph.D. Thesis, University of Hawaii, 1968. (In print)
6. McDougall, I. "Potassium-Argon Ages from Lavas of the Hawaiian Islands." Geological Society of America Bulletin, 75, p. 589ff, 1953.
7. Amirkhanov, K. I., S. B. Brandt, and E. N. Bartnitsky. "Radiogenic Argon in Minerals and its Migration." Annals of the New York Academy of Science, 91, pp. 235-275, 1961.
8. Evernden, J. F., G. H. Curtis, R. W. Kistler, and J. Obradovich. "Argon Diffusion in Glauconite, Microcline, Sanidine, Leucite and Phlogopite." American Journal of Science, 258, pp. 583-604, October 1960.
9. Fechtig, H., W. Gentner, and P. Lammerzahl. "Argonbestimmungen an Kaliummineralien--XII Edelgasdiffusionsmessungen an Stein- und Eisenmeteoriten." Geochimica et Cosmochimica Acta, 27, pp. 1149ff, 1963.
10. Naughton, J. J. "Possible Use of Argon-39 in the Potassium-Argon Method of Age Determination." Nature, 197, pp. 661-663, 1963.
11. Carslaw, H. S. and J. C. Jaeger. Conduction of Heat in Solids (2nd edition). Clarendon Press, Oxford, 1959.
12. Reichenburg, D. "Properties of Ion Exchange Resins in Relation to Their Structure. III. Kinetics of Exchange." Journal of the American Chemical Society, 75, p. 589ff, 1953.
13. Kalbitzer, S. "The Application of the Linear Heating Technique to the Diffusion of Rare Gases in Solids." Earth and Planetary Science Letters, 3, pp. 317-320, 1967.

1. S. H. Bauer, *et al.*, *Journal of Polymer Science*, **10**, 105 (1953).
2. S. H. Bauer, *et al.*, *Journal of Polymer Science*, **10**, 115 (1953).
3. S. H. Bauer, *et al.*, *Journal of Polymer Science*, **10**, 125 (1953).
4. S. H. Bauer, *et al.*, *Journal of Polymer Science*, **10**, 135 (1953).
5. S. H. Bauer, *et al.*, *Journal of Polymer Science*, **10**, 145 (1953).
6. S. H. Bauer, *et al.*, *Journal of Polymer Science*, **10**, 155 (1953).
7. S. H. Bauer, *et al.*, *Journal of Polymer Science*, **10**, 165 (1953).
8. S. H. Bauer, *et al.*, *Journal of Polymer Science*, **10**, 175 (1953).
9. S. H. Bauer, *et al.*, *Journal of Polymer Science*, **10**, 185 (1953).
10. S. H. Bauer, *et al.*, *Journal of Polymer Science*, **10**, 195 (1953).
11. S. H. Bauer, *et al.*, *Journal of Polymer Science*, **10**, 205 (1953).
12. S. H. Bauer, *et al.*, *Journal of Polymer Science*, **10**, 215 (1953).
13. S. H. Bauer, *et al.*, *Journal of Polymer Science*, **10**, 225 (1953).

14. MacDonald, G. A. and T. Katsura. "Chemical Composition of Hawaiian Lavas." *Journal of Petrology*, 5, pp. 82-133, February 1964.
15. United States Department of the Interior, Geological Survey, Laboratory Report No. 66DC-7, February 15, 1966.
16. MacDonald, G. A. "Petrography of the Waianae Range, Oahu" in H. T. Stearns, "Supplement to the Geology and Groundwater Resources of the Island of Oahu, Hawaii," *Hawaii Division of Hydrography Bulletin*, 5, pp. 63-91, 1940.
17. Reynolds, J. H. "High Sensitivity Mass Spectrometer for Noble Gas Analysis." *The Review of Scientific Instruments*, 27, pp. 928-934, 1956.
18. Alpert, D. and R. S. Burlitz. "Ultra High Vacuum. II. Limiting Factors in the Attainment of Very Low Pressures." *Journal of Applied physics*, 25, pp. 202-209, 1954.
19. Alpert, D. "New Developments in the Production and Measurement of Ultra High Vacuum." *Journal of Applied Physics*, 24, pp. 860-876, 1953.
20. Hamilton, E. I. Applied Geochronology. Academic Press, New York, 1965.
21. Stearns, H. T. and K. N. Vaksvik. "Geology and Groundwater Resources of Oahu, Hawaii." *Hawaii Division of Hydrography Bulletin*, 1, p. 67, 1935.
22. Lanphere, M. A. and G. B. Dalrymple. "Simplified Bulb Tracer System for Argon Analyses." *Nature*, 209, pp. 902-903, February 1966.
23. Barnes, I. L. Personal communication.

14. Macdonald, J. A. and T. Lawrence. "Physical composition of Hawaiian lavas." *Journal of Geology*, 5, pp. 82-117, February 1904.

15. United States Department of the Interior, Geological Survey, Laboratory Report No. 602, February 17, 1906.

16. Schuchert, C. A. "Petrology of the Hawaiian Islands, with a description of the lavas, and a study of the geology and geodesy of the island of Oahu, Hawaii, Division of Geology Bulletin, 5, pp. 53-81, 1910.

17. Schuchert, C. A. "The Hawaiian Islands, a geodesic survey, and a study of the geology of the Hawaiian Islands, Division of Geology Bulletin, 5, pp. 82-117, 1910.

18. Schuchert, C. A. and R. S. Burrill. "The Hawaiian Islands, a geodesic survey, and a study of the geology of the Hawaiian Islands, Division of Geology Bulletin, 5, pp. 82-117, 1910.

19. Schuchert, C. A. "The Hawaiian Islands, a geodesic survey, and a study of the geology of the Hawaiian Islands, Division of Geology Bulletin, 5, pp. 82-117, 1910.

20. Schuchert, C. A. *Applied Petrology*. Academic Press, New York, 1907.

21. Schuchert, C. A. and R. S. Burrill. "Geology and Geodesy of the Hawaiian Islands, Hawaii, Division of Geology Bulletin, 5, pp. 82-117, 1910.

22. Schuchert, C. A. and R. S. Burrill. "Geology and Geodesy of the Hawaiian Islands, Hawaii, Division of Geology Bulletin, 5, pp. 82-117, 1910.

23. Schuchert, C. A. and R. S. Burrill. "Geology and Geodesy of the Hawaiian Islands, Hawaii, Division of Geology Bulletin, 5, pp. 82-117, 1910.

24. Schuchert, C. A. and R. S. Burrill. "Geology and Geodesy of the Hawaiian Islands, Hawaii, Division of Geology Bulletin, 5, pp. 82-117, 1910.

VI. Acknowledgments

Thank you:

Dr. John Naughton, for your patience and your advice;

John Gramlich, for making impossible things possible;

Clyde Noble, for patiently answering all those ???;

Sister Mary, for the loan of your drawing equipment;

Larry, for "not helping";

and most of all, thank you:

Dr. I. L. Barnes, for, really making the whole thing and
a lot more possible;

Amy, for the loan of your typewriter and pen and for making
the whole thing bearable;

E., for -----;

Mom, Dad, P. and V., for being around.

VI. Acknowledgments

Thank you

Dr. John Vanhook, for your patience and your advice;

John Gramlich, for making impossible things possible;

David Smith, for patiently answering my questions;

Stationery, for the loan of your typewriter;

TYPE-ERASE

and most of all, thank you

Mr. J. J. Barnes, for his help in the whole thing and

for his cooperation.

But, for the loan of your typewriter and for making

the whole thing possible;

Yours truly,

John Vanhook, Jr. and John Vanhook, Sr.